Integrating Natural and Engineered Genetic Variation to Decode Regulatory Influence on Blood Traits

Authors: Manuel Tardaguila[1,2]*, Dominique Von Schiller[1], Michela Colombo[2], Ilaria Gori[2], Eve L. Coomber[1], Thomas Vanderstichele[1], Paola Benaglio[2], Chiara Chiereghin[2], Sebastian Gerety[1], Dragana Vuckovic[2], Arianna Landini[2], Giuditta Clerici[2], Patrick Albers[1], Helen Ray-Jones[3], Katie L. Burnham[1], Alex Tokolyi[1], Elodie Persyn[4,5,14], Mikhail Spivakov[4], Vijay G. Sankaran[6], Klaudia Walter[1], Kousik Kundu[1,13], Nicola Pirastu[2], Michael Inouye[4,5,7,8,9,13], Dirk S. Paul[4,10,13], Emma E. Davenport[1], Pelin Sahlén[11], Stephen Watt[1], Nicole Soranzo[1,2,12,13,14,**]

Abstract

Understanding the functional consequences of genetic variants associated with human traits and diseases —particularly those in non-coding regions—remains a significant challenge. Here we use analyses based on natural genetic variation and genetic engineering approaches to dissect the function of 94 non-coding variants associated with haematological traits. We describe 22 genetic variants with impact on haematological variation through gene expression. Further, through in-depth functional analysis, we illustrate how a rare, non-coding variant near the *CUX1* transcription factor impacts on megakaryopoiesis through modulation of the *CUX1* transcriptional cascade. With this work we advance the understanding of the translational value of association studies for variants implicated in blood and immunity.

[1] Wellcome Sanger Institute, Wellcome Genome Campus, Hinxton, UK.
[2] Imperial College London, School of Public Health, Faculty of Medicine, London, UK
[3] MRC Laboratory of Medical Sciences, Faculty of Medicine, Imperial College, London, UK
[4] Victor Phillip Dahdaleh Heart and Lung Research Institute, University of Cambridge, Cambridge UK
[5] Cambridge Baker Systems Genomics Initiative, Department of Public Health and Primary Care, University of Cambridge, Cambridge, UK
[6] Division of Hematology/Oncology, Boston Children's Hospital and Department of Pediatric Oncology, Dana-Farber Cancer Institute, Harvard Medical School, Boston, Massachusetts, USA
[7] British Heart Foundation Centre of Research Excellence, University of Cambridge, Cambridge, UK
[8] Health Data Research UK Cambridge, Wellcome Genome Campus and University of Cambridge, Cambridge, UK
[9] Cambridge Baker Systems Genomics Initiative, Baker Heart and Diabetes Institute, 75 Commercial Rd, Melbourne 3004, Victoria, Australia
[10] Centre for Genomics Research, Discovery Sciences, BioPharmaceuticals R&D, AstraZeneca, Cambridge, UK
[11] Royal Institute of Technology - KTH, School of Chemistry, Biotechnology and Health, Science for Life Laboratory, Stockholm, Sweden
[12] Department of Haematology, University of Cambridge, Cambridge Biomedical Campus, Cambridge, UK.
[13] British Heart Foundation Cardiovascular Epidemiology Unit, Department of Public Health and Primary Care, University of Cambridge, Cambridge UK
[14] National Institute for Health Research Blood and Transplant Research Unit in Donor Health and Genomics, University of Cambridge, Cambridge, UK
* Corresponding authors

Introduction

Genome-wide association studies (GWAS) of haematological traits have yielded thousands of high quality variant to phenotype associations that underpin key aspects of blood homeostasis and immune response[1,2]. Population-scale quantitative trait loci (QTL) initiatives in immune cells[3] and whole blood[4] have been instrumental in explaining how GWAS supported genes modulate blood traits in health and disease[2,5]. It has been estimated that up to 90% of the GWAS associations for haematological phenotypes lie in the non-coding genome[2], slowing down efforts to identify target genes and to elucidate the mechanisms by which these variants exert their effects. Identifying transcriptional regulators underpinning such genetic effects is critical to enable progress into pharmaceutical intervention, as recently illustrated by the approval of CRISPR/Cas9 ex-vivo therapies (Casgevy[6]) to treat sickle cell disease and Beta-Thalassemia[6]. In this first case study example, the accumulation of non-coding variants that control foetal haemoglobin levels through the expression of the transcriptional repressor BCL11A[7,8] informed the identification of an erythroid-specific enhancer that could be targeted to thus successfully ameliorate the symptoms of both diseases[8].

Variant-to-function studies are hindered by several factors including difficulties in scaling-up functional validation techniques, in prioritising variants within extended blocks of variants in linkage disequilibrium (LD) and in linking unequivocally genetic variants to their candidate effector genes. Functional validation of haematological variants has relied on expression QTL (eQTL)[4,5] studies and high-throughput experimental screenings such as Massively Parallel Reporter Assays (MPRA)[9–11], CRISPR-Cas9[12] and CRISPR interference (CRISPRi)[13] assays. Despite the valuable insights provided by these approaches, important challenges remain. The functional impact of hundreds of rare non-coding GWAS variants (RNVs) increasingly uncovered by the use of denser imputation panels and whole genome sequencing (WGS)[14] has not been fully addressed, as eQTL studies use under-powered methods for rare variation and few MPRA[10] and CRISPRi[13] screenings have included them in their design. In addition, little has been done to reconcile the differences between *in vivo* results from expression studies and *in vitro* results from screenings taking into account that the latter often do not assay variants in their native chromatin context (episomal MPRAs[10]) and tend to produce experimental artifacts (MPRA[15] and CRIPSRi[16]). Furthermore, phased WGS data that allows to break down the effect of different haplotypes is often lacking in eQTL studies. Finally, very few screenings have assessed variants in cell contexts that are relevant for the blood phenotypes mapped to the variants[17].

Here we have addressed the function of 94 rare non-coding variants (RNVs) associated with haematological traits using a MPRA for enhancer activity and an analysis for differential gene expression (DE) and alternative transcript usage (ATU) in a large collection of samples with whole blood RNA-seq and phased WGS data. After extensive manual curation we identify 22 variants with direct regulatory evidence to genes robustly associated with blood traits. Finally, we have carried out an in-depth functional validation of one of these variants elucidating a molecular mechanism that recapitulates the GWAS association.

Results

Variant prioritisation and MPRA in hematopoietic cell lineages

To identify a set of variants to perform our study we started from 12,181 loci associated with 29 different blood phenotypes from a GWAS study conducted by our group[2]. These haematological traits (**Table S1**) encompass a broad range of clinical indices used to evaluate the state of the erythrocyte, megakaryocyte, monocyte and lymphoid lineages in blood. From the 178,890 variants contained in 95% fine mapping credible sets, we applied sequential filters. We first restricted the dataset to rare variants (minor allele frequency [MAF] ≤ 1%) leaving 5,813 variants. Next we retained only rare non-coding variants, defined using the most severe consequence in Variant Effect Predictor (VEP), leaving 5,248 variants. We then selected variants with at least one trait association fine-mapped with a posterior probability (PPFM) ≥ 0.9 narrowing the set to 196 variants and finally we prioritised variants with high effect sizes (beta < first or > third quartile of standardised trait distribution) (**Figure 1A-C and Methods**). Following these steps we identified a set of 123 rare non-coding variants (RNVs) meeting all criteria, henceforth named 'index variants' (**Figure 1A** and **Table S2**). These index variants exhibited significantly higher effect sizes compared to reported heterozygous blood ClinVar/HGMD pathogenic variants[2] (p value = 0.009, *Wilcoxon test*). Notably, 95% of index variants remained significantly associated with at least one blood trait after conditioning on common variants, in contrast to other selection approaches that prioritize subsets whose signal is ultimately driven by LD with nearby common variants[18]. Furthermore, index variants had significantly higher orthogonal prioritisation scores; including combined annotation dependent depletion ([CADD][19]), NCBoost[20], and genomic non-coding constraint of haploinsufficient variation ([Gnocchi][21]) compared to other tiers of RNVs (**Figure 1C**).

Out of the 123 index variants, 94 were incorporated into an MPRA library design for enhancer activity[15,22] alongside positive and negative controls selected from previous studies[9,23]. To account for sequence context effects[24], each variant allele was synthesised within five partially overlapping tiles tagged with unique barcodes and cloned into an MPRA reporter vector (**Methods**). The resulting MPRA library (19,050 oligos) was transfected in seven different replicates into four cancer cell lines used as models of blood cell types: K-562 (chronic myeloid leukaemia, a model erythroid cell), CHRF-288-11 (acute megakaryoblastic leukaemia, a model for megakaryocytes), HL-60 (acute myeloid leukaemia, a model neutrophil line) and THP-1 (acute monocytic leukaemia, a model for monocytes) (**Figure 2A**). To quantify enhancer activity and allele specific expression we employed MPRAmodel[25] estimating log2 Fold Change(log2FC) and log2 Allelic Skew, (log2AS) per each tile, variant and cell type (**Table S3**). We performed a meta-analysis across tiles to obtain a single value of log2FC and log2AS per variant and cell type as described in[10](**Table S4**). The directionality of the log2AS positive controls showed high concordance with a prior MPRA study in K-562 cells[9] (R^2 = 0.821, **Supplementary Figure 1B**). We identified 43 variants that significantly impacted the activity of enhancer sequences and labelled them as MPRA positive (**Figure 2A-B, Supplementary Figure 1C, Table S4 and S6**). The high proportion of MPRA positive variants (45.7%) is consistent with previous findings that high PPFM variants are enriched in MPRA activity[10]. Among the four cell lines tested, THP-1 cells displayed the lowest number of MPRA positive variants (4, **Supplementary Figure 1C**) possibly due to them being refractory to nucleofection[26] as they also had the lowest % of GFP positive cells after transfection (median values 55.5 and 6.8 for CHRF-288-11 and THP1 cells, respectively, p value = 0.01, *Wilcoxon test*).

Among the 43 MPRA positives, 25 were specific to a single cell type while 14 and 4 were shared across two and three cell types respectively (**Figure 2C, Supplementary Figure 1C**). We

observed high correlation (Pearson correlation > 0.9) in log2FC and log2AS for the MPRA positive variants shared by the K-562 and HL-60 cells (**Figure 2D, Supplementary Figure 1D**) possibly reflecting their common myeloid leukaemia origin[27,28]. To investigate the factors influencing log2FC activity we incorporated cell-matched sequence features obtained from Enformer[29,24] into our set GWAS parameters and scores and applied lasso regression[24]. Among the GWAS parameters, MAF emerged as predictive factor in K-562, CHRF-288-11 and HL-60 cells (**Figure 2E**), suggesting that rare variants in the lower spectrum of allele frequency in our study (MAF < 0.01) tended to have higher values of Log2FC (**Supplementary Figure 1E**). In addition, higher CADD scores were predictive of higher Log2FC variants in the HL-60 cell line (**Figure 2E**). CHIP-seq data further revealed that motifs occupied by classical activating transcription factors (*STAT1*, *STAT2*) predicted higher LogFC values whereas known repressors and insulators (*CTCF, RFX1*) predicted negative LogFC values (**Figure 2E**). Altogether, these findings indicated that the MPRA captured the capacity of multiple index variants to impact the activity of enhancer sequences, reinforcing their potential functional relevance.

Population survey of RNA expression in healthy volunteers supports variant effects mediated by transcription

To assess regulatory impact of the index variants in their native chromatin context we used two bulk RNA-seq datasets (**Table S5**). First, the INTERVAL RNA-seq study[30], that includes gene and transcript quantification from whole blood samples of 2,971 samples with matched WGS data (15x). Overall, we identified heterozygous carriers for 88 of the 94 MPRA screened variants with a median of 40 carriers per variant. Since the traditional eQTL approach[4] is under-powered for variants with low allele counts, we employed a more calibrated differential gene expression analysis (DE), accounting for an array of experimental covariates to test for differences in expression levels between *wildtype* and heterozygous carriers of rare alleles at index variants (**Methods**). Additionally, we explored regulatory mechanisms beyond gene expression control by testing for alternative transcript usage (ATU), defined as changes in the relative abundance of transcripts expressed for each gene[31]. To model ATU we used an additive log ratio approach that accounts for its compositional nature incorporating all the experimental covariates used in the DE analysis (**Methods**).

We detected evidence for DE or ATU at 42 of the 88 variants, involving 60 genes (**Figure 3A, and Table S5**). Among these, 23 variants (involving 29 genes) exhibited only DE effects, 11 (involving 11 genes) had only ATU effects and 8 displayed both types of regulation (affecting 14 genes with DE, 4 genes with ATU and 5 genes with simultaneous DE and ATU, **Table S5**). Eight of the 20 ATU genes harbour splicing QTLs (sQTL) signals in whole blood in the GTEx Project[32], but implicating common variants (MAF > 1%) that were conditionally independent from the ones assayed here (r^2>0.7, EUR population, window size 0.5 Mb, **Methods**). In the INTERVAL QTL repository[30] we identified three of the ATU variants as sQTLs for the correspondent genes and for an additional 11 ATU genes we found independent common sQTLs. This suggests complex modes of regulation at the transcript level for ATU genes (**Supplementary Figure 2A)**. One of the ATUs involved the synonymous cryptic splicing variant rs150813342 in *GFI1B*, a transcriptional repressor and key regulator of platelet and red blood cell development (**Supplementary Figure 2B**). Editing the same variant using CRISPR/Cas9 in K-562 cells induced similar transcript usage changes[33].

To investigate the contribution of individual cell types, we also analysed DE and ATU in three separate immune cell isolates (monocytes, neutrophils and naive CD4+ T-cells) from the BLUEPRINT human variation panel[3]. Of the 88 variants examined in INTERVAL, 25 had at least one heterozygous carrier in the 196 BLUEPRINT donors (median number of 5 carriers per

variant). We detected evidence for DE or ATU at 10 of the 25 variants, involving 11 genes (**Figure 3A** and **Table S5)**. Among these, 4 variants (affecting 4 genes) exhibited only DE effects, 3 (involving 3 genes) had exclusively ATU effects and 3 showed both types of regulation (affecting one gene with DE, one gene with ATU and two genes with simultaneous DE and ATU). Among the ten BLUEPRINT DE/ATU variants, five were shared with the INTERVAL whole blood analysis with 3 implicating the same genes. In 4 of the remaining 5 cases, regulatory effects were detected exclusively in one BLUEPRINT cell type (**Figure 3A** and **Table S5**). Overall, the RNA-seq supported multiple MPRA positives with some differences that we explore further.

Regulatory landscapes defined by *in vivo* and *in vitro* studies

We combined evidence from the MPRA and RNAseq (DE/ATU) experiments to assess how the multiple lines of evidence converge towards a mechanistic interpretation of each association, categorising the tested variants into four groups: 18 double-positive variants (showing regulatory effects in both MPRA and RNAseq), 22 MPRA+/RNA- variants, 29 MPRA-/RNA+ and 19 MPRA-/RNA- variants (**Figure 3B** and **Table S6**).

In the double-positive set we investigated the concordance in the direction of the effect allele between MPRA Allelic Skew and DE and found moderate agreement (8/14, **Methods**). For the 22 *MPRA +/ RNA-* variants (**Figure 3B**), we hypothesised that the lack of RNA evidence was driven by insufficient statistical power in the DE/ATU particularly for variants with lower allele frequencies. Indeed, variants with no RNA effect had a significantly lower number of carriers than DE and/or ATU variants (p value = 0.045, *Wilcoxon test*, **Figure 3C**). Next we examined the 29 *MPRA-/RNA+* variants to determine whether they were enriched in ATU cases that might escape MPRA detection of enhancer activity. However, there was no significant difference in the distribution of ATU events between double-positive and *MPRA-/RNA+* variants (p value =1, *Chi square test,* **Figure 3B** and **Table S6**). We then applied lasso regression to identify sequence based features predictive of the MPRA-/RNA+ class compared to double-positive variants (**Methods**). We found three CHIP-seq motifs in K-562 cells (*E2F, RLF* and *BCLAF1*) associated with the MPRA-/RNA+ class (**Figure 3D**). Notably, *E2F* and *RLF* (**Supplementary Figure 2C**) exhibited very low expression levels in K-562 cells, suggesting that a some of the MPRA-/RNA+ variants might affect motifs of transcription factors that are weakly expressed in the cell lines used for the MPRA.

To annotate candidate effector genes underpinning the genetic associations we integrated data from the GeneBass[34] and OpenTargets[35] databases and conducted a comprehensive literature search, (**Supplementary Figure 3** and **Table S6**). For variants with regulatory evidence in the RNA-seq experiments we used all the DE/ATU genes whereas for RNA negative variants, we considered all genes tested in the DE/ATU analysis. In total, we annotated genes for 76 of the 88 variants. We then leveraged phased WGS (unavailable at the time of the MPRA assay design) to identify cases where the association could be explained by a nearby coding variant (labelled as "coding proxy") in high LD with the index variant. Fourteen variants had at least one coding proxy variant (r^2 range 0.26-0.97); however we observed evidence for regulatory activity at 7 of these, suggesting that either the index or the coding proxy variant could be causal (**Supplementary Figure 4D)**. Furthermore, using the haplotype resolved information from the same WGS data, we identified four instances where other non-coding variants (labelled as "regulatory proxy") in high LD with the index variant (r^2 range 0.51-0.85) were driving the DE/ATU expression phenotype (**Supplementary Figure 4E**). Additionally, we flagged ten variants where the regulatory effects are likely mediated in cell types or tissues different from the ones used here (labelled as "other tissue", **Supplementary Figure 4F**), and seven cases where

the regulated genes were not a solid biological candidate for the GWAS phenotypes (labelled as "other gene"). Overall, our curation effort results in a high-confidence set of 22 variants for which we can formulate robust hypotheses linking the regulated genes to the blood phenotypes ('GeneBass, Open Targets or literature support' label, **Figure 3E** and **Table 1**). Of these, 11 implicated DE events (**Supplementary Figure 4A**), 7 ATU events (**Supplementary Figure 4B**) and 4 had both types of regulation (**Supplementary Figure 4C**). In addition, five had been previously described as eQTLs for the same genes by the eQTLGen[4] and/or the BLUEPRINT[3] consortia and 1 as an sQTL in the INTERVAL RNA-seq initiative[30], **Table 1**. Notably, 12 of the 22 'GeneBass, Open Targets or literature support' variants were MPRA positive in contrast to none of the regulatory proxy variants demonstrating the capacity of the MPRA to capture true biological effects.

Regulation of megakaryocytic size and maturation by *cis* variation in *CUX1*

We validated the double-positive variant rs139141690, which was MPRA positive in K-562 cells and downregulated the gene *CUX1*. *CUX1* encodes a transcription factor essential for hematopoietic stem cell (HSC)[36] maintenance (**Figure 4A and Table S4-5**). The GWAS phenotypes associated with the variant (e.g. mean platelet volume) align with findings observed in murine *knock-downs* of *CUX1*[36]. The variant is located in a region of accessible chromatin that interacts with the promoter of *CUX1* in the megakaryocyte lineage (**Figure 4A**). Motif analysis predicts a *PU.1* site in the reference sequence that is transformed into a *FOXM1* by the alternative A allele, while CHIP-seq in whole blood shows the occupancy of the motifs by both TFs (**Supplementary Figure 5A,B** and **Methods**). Moreover, complementing our RNA-seq analysis with a gene set enrichment analysis (GSEA) in the INTERVAL whole blood carriers revealed a significant enrichment of the *HSC homeostasis* and *Blood coagulation* pathways in heterozygous carriers of the variant (**Supplementary Figure 5C**).

We used Genome engineering-based Interrogation of Enhancers (GenIE)[12] to assess whether CRISPR/Cas9 introduced unique deletion profiles (UDPs) and rs139141690 'A/A' allele significantly affected the expression of *CUX1*[12,37]. We assayed rs139141690 in three of the MPRA cancer cell lines (K-562, HL-60 and THP-1) and a human induced pluripotent cell line (hiPSC, Kolf2)[12]. Multiple UDPs and the rs139141690-A allele showed a significant decrease in the abundance of *CUX1* transcripts when compared to the wildtype allele in K-562 cells, recapitulating the decrease in *CUX1* expression observed *in vivo* (**Figure 4B)**. Next, we explored the role of rs139141690 in the megakaryocyte lineage by differentiating K-562 cells to megakaryocyte-like CD41+ (*ITGA2B* gene, megakaryocyte surface marker) cells using PMA[33]. First, we engineered three sets of isogenic K-562 lines carrying respectively: i) the reference allele ('G/G' clones), ii) the alternative allele ('A/A' clones) and iii) a specific 80 bp deletion spanning the SNP and covering all the significantly active UDPs from the GenIE ('80 bp del' clones) (**Figure 4C**). We monitored the changes in the cell surface abundance of CD235 (*GYPA* gene, erythrocyte surface marker) and CD41 by flow cytometry. The A/A clones accumulated more intermediate $CD235^{+}CD41^{+}$ cells but had fewer terminally differentiated single positive CD41 cells while the "80 bp del" clones reached high percentages of them faster than any other genotype (**Figure 4D** and **Methods**). These findings confirmed the capacity of rs139141690 to affect megakaryocyte differentiation *in vitro*.

To explore the regulatory mechanism of rs139141690 on *CUX1* we performed a K-562 differentiation experiment jointly capturing RNA expression and open chromatin landscapes at single cell level (**Figure 5A**). In this experiment we included two additional clone lines: one heterozygous for rs139141690 ('A/G') and one carrying a shorter deletion that spanned the PU.1 binding site impacted by the variant ('16 bp del', **Supplementary Figure 5A**). We

barcoded each clone line using a lentivirus library and recovered 11,250 genotyped cells, which clustered into 13 different groups (**Figure 5A, B** and **Methods).** We focused on two clusters that accumulated over time with treatment: cluster 3, enriched for co-expression of megakaryocyte markers and haemoglobin genes, and cluster 1, with high *ITGA2B* expression, and additionally, high levels of the polyploidization genes indicative of late-stage megakaryocyte maturation (**Figure 5B-C** and **Supplementary Figure 5D**).

We then analysed the impact of the four mutations relative to 'G/G' cells in gene expression (differential expression, DE) and in chromatin accessibility (differential accessibility, DA) (**Methods** and **Table S8**). The heterozygous genotype showed four DE genes and three DA peaks connected to the AKT/mTOR signalling pathway (**Figure 5D)**. In contrast, the 'A/A' genotype showed multiple DE genes belonging to the AKT/mTOR pathway, as well as *EZH2* (a "polyploidization gatekeeper"[38]), its target *XRCC2* and an upregulation of *FYB1* implicated in the production of platelets of abnormal volume[39]. Crucially, only the 'A/A' genotype exhibited significant downregulation of the *CUX1* gene concomitant with a decrease in chromatin accessibility in the peak that harbours the variant (**Figure 5D-E** and **Table S8**). Moreover, *CUX1* target genes were overrepresented in the DE genes (p value = 0.033, 'A/A' vs 'G/G' genotypes, *ORA analysis,* **Methods**) (**Figure 5D)**. DA analysis also identified significant changes in peaks linked with the genes *EZH2* and *XRCC2* (**Figure 5D** and **Table S8**). The two deletions produced complementary results; the long deletion was associated with differential expression of multiple genes involved in megakaryocyte fate (e.g. *TBXAS1*, *TBXA2R*) and platelet volume (e.g. *ITGA2B*, *TUBB1*), while the short deletion was associated with fewer DE genes with concordant direction of effect on gene expression (**Figure 5D**). In both deletions, *CUX1* target genes were significantly overrepresented in DE genes despite no change in *CUX1* expression (p value = 0.002 and p value = 8.95 $x10^{-5}$, Del16 vs G/G and Del80 vs G/G genotypes respectively, *ORA analysis*) (**Figure 5D)**. Finally, to connect the cellular phenotypes observed at the single-cell level with GWAS-associated traits for the variant, we used flow cytometry parameters FSC-A and SSC-A as proxies. We observed that "80-bp del" and 'A/A' cells were significantly bigger CD41 single positive cells after 72 hours of treatment when compared to 'G/G' cells (p value < 0.0001, *Wilcoxon test*) (**Figure 5F**). Altogether these results recapitulate the increase in mean platelet volume observed in the GWAS.

Discussion

A previous comprehensive association analysis of blood indices by our group discovered 16,900 conditionally independent trait-variant associations[2]. Here we leveraged the GWAS parameters to select a group of 94 RNVs for functional follow-up. Our work builds upon and extends previous efforts to i) prioritize causal variants within extended linkage disequilibrium (LD) blocks, including a detailed examination of the experimental and GWAS evidence to exclude cases where other rare variants in LD drive the associations, ii) identify regulated genes that are strong candidates for the changes in blood traits, iii) utilize cellular models relevant to the GWAS associations and iv) assess the propagation of the impact of non-coding variants affecting transcription factors to their target genes[13]. Importantly, 16 out of the 22 variants for which we propose a mechanism had no prior *in vivo* evidence of regulatory effect on the indicated genes.

Our in-depth validation has focused on rs139141690 and *CUX1*. This variant was recently assayed in an independent CRISPRi study, which showed a CRISPRi-dependent *CUX1* downregulation for the region but failed to reveal a significant effect of the SNP in K-562 cells[13]. Despite its higher throughput, this approach does not provide a genotyped readout (sgRNA detection is taken as a proxy for successful editing) and is therefore susceptible to false negatives.

We propose that our approach, using genotyped clones and subsequent differentiation in a megakaryocyte model is better tailored to reveal the effect of the variant. Our multiome experiment provided key insights into the mechanism of rs139141690, demonstrating a causal relationship between *CUX1* expression and chromatin accessibility in the region that harbours the variant. Moreover, it revealed the broad dysregulation of AKT/mTOR related genes consistent with the role of *CUX1* in the *PI3K/AKT* pathway in human cancers[40]. Finally, we hypothesise a plausible link between the downregulation of *EZH2* in cluster 3 and the accumulation of double-positive $CD235^{+}CD41^{+}$ cells as *EZH2* inhibition has been shown to block polyploidization and proliferation in megakaryocyte differentiation[38]. Collectively, these results suggest the presence of a genetic program regulating platelet volume controlled by the hub of TF motifs in which the variant resides.

This study advances the functional characterization of high impact rare non-coding GWAS variants that are often overlooked due to the inherent complexities in their analysis and the intricacies of the regulatory mechanisms. Overcoming these challenges is crucial, as our findings highlight the unique mechanistic insights into target specificity and regulatory modulation that such variants can provide.

.

Acknowledgements

Acknowledgements: Tristram Bellerby, Mathew Mayho, Jeremy Schwartzentruber, Sarah Cooper, Andrew Bassett from the Wellcome Sanger Institute. Cecilia Dominguez-Conde, Davide Bolognini and Edoardo Giacopuzzi from the HT Population and Medical Genomics centre. Alessio Palini, Nicolò Panini, Silvia Bombelli in the HT Flow Cytometry Applications Resource unit and Clelia Peano, Eugenia Ricciardelli, Javier Cibella, Fabio Simeoni, Niccolò Alfano, Paolo Ferrari and Luigi Lamparelli in the HT Genomic Facility.

This work has been funded by BHF Cambridge Centre for Research Excellence RE/18/1/34212, the Chan Zuckerberg foundation and MIUR/MEF through Fondazione Human Technopole. M.I. and E.P. were supported by core funding from the British Heart Foundation (RG/18/13/33946: RG/F/23/110103), NIHR Cambridge Biomedical Research Centre (NIHR203312) [*], BHF Chair Award (CH/12/2/29428), and by Health Data Research UK, which is funded by the UK Medical Research Council, Engineering and Physical Sciences Research Council, Economic and Social Research Council, Department of Health and Social Care (England), Chief Scientist Office of the Scottish Government Health and Social Care Directorates, Health and Social Care Research and Development Division (Welsh Government), Public Health Agency (Northern Ireland), British Heart Foundation and the Wellcome Trust. M.I. was also supported by the UK Economic and Social Research 878 Council (ES/T013192/1). *The views expressed are those of the authors and not necessarily those of the NIHR or the Department of Health and Social Care.

RNA-seq in the INTERVAL study was funded as part of an alliance between the University of Cambridge and the AstraZeneca Centre for Genomics Research, and by the NIHR Cambridge Biomedical Research Centre (BRC-1215-20014). Participants in the INTERVAL randomised controlled trial were recruited with the active collaboration of NHS Blood and Transplant England (www.nhsbt.nhs.uk), which has supported field work and other elements of the trial. DNA extraction and genotyping were co-funded by the National Institute for Health and Care Research (NIHR), the NIHR BioResource (http://bioresource.nihr.ac.uk) and the NIHR Cambridge Biomedical Research Centre (BRC-1215-20014) [*]. The academic coordinating centre for INTERVAL was supported by core funding from the: NIHR Blood and Transplant Research Unit (BTRU) in Donor Health and Genomics (NIHR BTRU-2014-10024), NIHR BTRU in Donor Health and Behaviour (NIHR203337), UK Medical Research Council (MR/L003120/1), British Heart Foundation (SP/09/002; RG/13/13/30194; RG/18/13/33946), NIHR Cambridge BRC (BRC-1215-20014; NIHR203312) [*], and by Health Data Research UK, which is funded by the UK Medical Research Council, Engineering and Physical Sciences Research Council, Economic and Social Research Council, Department of Health and Social Care (England), Chief Scientist Office of the Scottish Government Health and Social Care Directorates, Health and Social Care Research and Development Division (Welsh Government), Public Health Agency (Northern Ireland), British Heart Foundation and Wellcome. A complete list of the investigators and contributors to the INTERVAL trial is provided in Di Angelantonio et al[41]. The academic coordinating centre would like to thank blood donor centre staff and blood donors for participating in the INTERVAL trial.
*The views expressed are those of the authors and not necessarily those of the NIHR or the Department of Health and Social Care.

Conflicts of interest
M.I. is a trustee of the Public Health Genomics (PHG) Foundation, a member of the Scientific Advisory Board of Open Targets, and has research collaborations with AstraZeneca, Nightingale Health and Pfizer which are unrelated to this study. T.V. has received PhD studentship funding

from AstraZeneca. K.K and D.P. are current employees and stockholders of AstraZeneca. P.A. is a current employee of Glaxosmithkline.

Tables and Figures

Table 1. Variants with curated mechanistic hypotheses. *For the abbreviations see Table S1.*

Figure 1. Variant prioritisation strategy and MPRA controls and inter-replica variability. A) Prioritisation strategy and **B)** VEP most severe consequence for the variants in the different tiers. **C)** Values of the MAF, PPFM, Absolute effect size, CADD, Gnocchi and NCBoost scores across the different tiers. *MAF = minimum allele frequency, PPFM = Posterior Probability in the Fine Mapping. The comparisons correspond to the values of the 'index variants' versus the rest of the tiers, Wilcoxon test.*

Figure 2. MPRA screening. A) Design of the MPRA for enhancer activity and **B)** results after the meta-analysis. **C)** Sharing of MPRA positive variants between the cell types assayed. **D)** Pearson correlation coefficients for MPRA positive variants across K-562, CHRF-288-11 and HL-60 cells. THP-1 had too few shared MPRA positives to perform meaningful comparisons. **E)** Lasso regression on sequence features predictive of Log2FC.

Figure 3. RNA-seq study results and curation of screened variants derived from RNA Seq, MPRA and GenIE readouts. A) Variants with significant DE/ATU genes. **B)** Breakdown of the overlap between the results of the MPRA and the RNA-seq. **C)** Variants without any regulation detected in the RNA-seq had significantly lower carriers in our datasets. **D)**.'Lasso regression on sequence features predictive of belonging to double-positive variants as opposed to MPRA-/RNA+. **E)** Breakdown of the mechanistic and manual curation labels by the results of the MPRA and the RNA-seq study.

Figure 4. rs139141690-A downregulates the hematopoietic TF CUX1. A) Locus plot for the variant rs139141690 that downregulates *CUX1* in whole blood. The variant sits in an intron of *CUX1* and has PCHi-C and accessible chromatin evidence in the megakaryocytic and erythroid lineages. **B)** GenIE results for the *knock-in* (highlighted in green) and UDPs (rest of profiles, two representative ones highlighted in blue and orange) of rs139141690 in K-562 cells. The highlighted UDPs and the *knock-in* allele significantly decreased the abundance of the mRNA in the edited cells. **C)** Time course differentiation of the edited K-562 cells to $CD41^+$ cells. **D)** Variation in the abundance of the different populations in the differentiation. The percentages represent the mean for the observation of the three clones per genotype. On the bottom the -log10 p values for the genotype comparisons of cell type abundance in the ilr model (see **Methods**). *See Table S1 for all abbreviations.*

Figure 5. Single Cell multimodal analysis confirms the effects on gene expression and chromatin accessibility elicited by rs139141690-A that reveal a regulatory region with key effects on platelet size. A) Experimental design including the additional clone lines. **B)** U-MAP combining both sc-RNAseq and sc-ATACseq modality. To the right, changes in their relative abundance across time points and genotypes **C)** Expression of five sets of marker genes characterising key stages in the differentiation. The dashed lines indicate the separation of the clusters into 4 groups that we hypothesise correspond to the flow cytometry subgroups. **D)** DE and DA analysis in the clusters 3 and 1 for the comparisons of each genotype against wild type cells. Genes belonging to more than one of the highlighted groups are mixed coloured (e.g. *TBXAS1*). **E)**. Locus plot detailing the DE and DA changes in clusters number 1 and 3 for the *CUX1* gene. The cpm values express either the gene expression counts for *CUX1* gene or the ATAC-seq counts for the different peaks displayed. **F)** FSC-A and SSC-A analysis across the genotypes in K-562 $CD41^+CD235^-$ cells at 72 hours. *Cyt. = cytometry, Mye. = myeloid, Megak. = megakaryocyte, Hb = Haemoglobin, polyploid = polyploidization, cpm =counts per million. See Table S8 for*

Peak coordinates.

STAR methods

Experimental model and study participants

MPRA data

The MPRA raw fastq files will be uploaded to the European Nucleotide Archive (ENA) upon publication.

ENCODE K-562 expression data

We used processed RNA-seq count matrices from basal K-562 cells.[42]

INTERVAL and BluePrint data

The INTERVAL study data used in this paper are available to bona fide researchers from ceu-dataaccess@medschl.cam.ac.uk. The data access policy for the data is available at http://www.donorhealth-btru.nihr.ac.uk/project/bioresource. The RNA-seq data in the INTERVAL cohort have been deposited at the European Genome-phenome Archive (EGA) under the accession number EGAD00001008015 and are available at[43]. The UK Biobank genetic data used in this study were approved under application 82779 and are available to qualified researchers via the UK Biobank data access process. For the BluePrint data we used data from[5]. All data are freely available but managed by the BLUEPRINT Data Access Committee.

10X multiome data

The 10X multiome raw fastq files will be uploaded to the European Nucleotide Archive (ENA) upon publication.

Cell culture

K-562 (ATCC® CCL-243™, sex female), and HL60 (ATCC®CCL-240, sex female) cells were cultured as indicated by the distributor, 1x RPMI 1640 media with L-glutamine (Gibco Medium.: 52400025), supplemented with 10% FBS (Gibco, A31604-02) and 1x penicillin/streptomycin (Gibco, 15070-063). THP-1 (ATCC® TIB-202, sex male) were culture as indicated by the distributor, 1x RPMI 1640 media with L-glutamine, 2-mercaptoethanol (Sigma, M3148) was added to a final concentration of 0.05mM and supplemented with 10% FBS (Gibco, A31604-02) and 1x penicillin/streptomycin. CHRF-288-11 (sex male, a kind gift from Prof. Wilen H Ouwehand's lab) were cultured 1x RPMI 1640 media with L-glutamine, supplemented with 20% Horse Serum (Gibco 16050-122) and 1x penicillin/streptomycin. All the cell types were maintained up to a confluence of $1x10^6$ cells/ml and then reseeded at $1x10^5$ cells/ml.m, except for THP-1 that were reseeded at $3x10^5$ and cultured in a T75 flask in an upright position. Phoenix Ampho (ATCC, CRL-3213, sex female) cells were cultured in DMEM 10% fbs prior to viral infections.

Induced Pluripotent Stem Cell (iPSC) line Kolf2_c1 line (Wellcome Sanger Institute's Human Induced Pluripotent Stem Cell Initiative, sex male) was cultured in TeSR-E8 complete culture media (Stem Cell Technologies #05991) (37°C, 5% CO2) on 10ng/ml Synthemax-II (Corning

CLS3535) coated plates. Kolf2_c1 were thawed into TeSR-E8 + 10% CloneR (StemCell Technologies # 05888) and split at 70-80% confluence into TeSR-E8 + 10uM Y27632 Rock Inhibitor (StemCell Technologies #72302).

To differentiate K-562 cells to CD41+ cells, we seeded 100.000 cells/ml in IMDM + 10% FBS and cultured in presence of 5nM phorbol 12-myristate 13-acetate (PMA, Selleckchem) or DMSO for 16, 24, 48 and 72 hours.

Method details

Variant Annotation

The 178,890 variants in the 95% credible sets of the 29 blood indices from Vuckovic et al[2] were prioritised attending to MAF (1% threshold), Variant-Effect-Predictor (VEP)[44] Most Severe Consequence (MSC), Posterior Probability (PP) and effect size (scaled to amount of standard deviation units per trait[2]). The prioritised subset of index variants were below or equal 1% MAF, MSC non-coding, with at least one blood index association above or equal 0.9 PP and with an effect size for that association between the absolute minimum and first quartile (beta < Q1) or the third quartile and the absolute maximum (beta > Q3), **Figure 1A** and **Table S2**. We condensed the VEP MSC option[45] into coding and non-coding consequences. The coding group comprised the following labels: LOF (Loss Of Function, [splice_acceptor_variant, splice_donor_variant, stop_gained and frameshift_variant]), MISS (missense_variant), UTR5 (5_prime_UTR_variant), UTR3 (3_prime_UTR_variant) and SYN (synonymous_variant). The non-coding group comprised the following labels: INTRON (intron_variant), INTERGENIC (intergenic_variant), UPSTREAM (upstream_gene_variant), DOWNSTREAM (downstream_gene_variant), REGULATORY (regulatory_region_variant), TFBS (TF_binding_site_variant), SPLICE (splice_region_variant), OTHER (start_lost, stop_lost, inframe_deletion, inframe_insertion, stop_retained_variant and mature_miRNA_variant), NMD (NMD_transcript_variant) and NCT (non_coding_transcript_variant). PCHi-C data was downloaded from Javierre et al[46] (PCHiC_peak_matrix_cutoff5.tsv). ATAC-seq data[47] was for blood cell types was downloaded from[48] (29August2017_EJCsamples_allReads_500bp.bed and 29August2017_EJCsamples_allReads_500bp.counts.txt) and intersected with our variants.

MPRA Library design and cloning

We designed a library of 20,340 200-mer oligonucleotides that were synthesised by Twist Bioscience. The library covered 113 SNPs, each one assayed in five partially overlapping tiles, every tile having an alternative and reference allele version. Each reference or alternative allele tile was tagged by 15 unique 11 bp barcodes. The library included 7 enhancer and allelic skew positive controls and 8 enhancer positive controls from[47] and four sequences that showed no CRISPRa activity in Fulco et al[23] as negative controls. The structure of the 200-mers included two 15 bp amplification arms at each end to amplify subpools/bins of the library based in GC content, an 11 bp barcode, the restriction enzyme sites for *BamH*I and *KpnI* and 148 bp of candidate regulatory sequence to be assayed. The amplification PCRs (Primers 1-6 **Table S7**) were done with Kapa HiFi HS Ready Mix (Kapa Biosystems), using 20 ng input template and 50 ul final volume with the exception of the High GC bin in which 20 ul of KAPA2G GC Buffer (ROCHE) was added to a final volume of 100 ul. Next we performed a digestion with *ExoI* (NEB) to eliminate free primers and then purified the amplified fragments using Agencourt AMPure beads (Beckman Coulter).

We based the backbone vector for this assay on the hSTARR-seq_ORI vector[15] (Addgene

#99296) following the recommendations from Muerdter et al[15]. We added GFP to the vector by excising sgGFP from the pSTARR-seq_human vector (Addgene Plasmid #71509[49]) with an o.n. digestion with *AflII* and *Age*I (New England Biolabs, NEB) at 37°C and ligating it with hSTARR-seq_ORI vector digested in the same manner (T4 DNA ligase 16□ o.n. 3 to 1 molar ratio). Following an idea proposed in the Supplementary Figure 1 I) of Muerdter et al[15], we excised the polyA site from the hSTARR-seq_ORI GFP vector to be cloned back at a later stage of our library construction to separate the barcode and the candidate regulatory sequence. The excision was carried out by *Nae*I digestion of the vector (60' 10 Units of enzyme, NEB) and posterior blunt end ligation to obtain the hSTARR-seq_ORI GFP polyA MINUS vector. The excised SV40 poly (A) signal fragment was amplified (Primers 9-10 **Table S7**) and cloned in the pGEM T easy system (Promega).

The amplified subpools of the library and the hSTARR-seq_ORI GFP polyA MINUS vector were ligated using Gibson cloning (NEB). Briefly, the vector was linearized by PCR (Primers 7-8 **Table S7**) and subsequently we carried out a digestion with *DpnI* and *BamH*I (NEB) to degrade the circular template. The ligation in Gibson mix was done with 100 ng of the linearized vector and a molar insert:vector ratio of 2:1 for each of the bins. The ligations were purified with Agencourt AMPure beads and eluted in 20 ul of Elution buffer diluted 1/10 in nuclease-free water and 10 ul of each were then used to electroporate electrocompetent E. coli bacteria (NEB) at 2000 V 25 uF 200 Ohm. We performed serial dilutions for each of the bins to ascertain the yield in colony-forming units (CFU) and aimed to keep a ratio of at least 100 CFU per oligo element. The individual colonies in each bin were lysed and the plasmids corresponding to each bin were purified using the Qiagen maxi prep kit (cat. 12162). This intermediate step in the library construction (PolyA Minus library) was sequenced to check the barcode - candidate regulatory sequence association and the design dropout rate. Briefly, we amplified 25 ngr of each of the poly (A) minus library bins (Medium GC, High GC and Low GC content) with oligos 11 and 19 (**Table S7**) for 15 cycles with annealing and extension done at 72°C in a combined step for 1'. The libraries were then quantified with KAPA Illumina SYBR Universal Lib Q. Kit. (Roche), adjusted at 4nM and pooled together for a final volume of 40 ul. The samples were subsequently sequenced in a MiSeq (MiSeq Reagent Kit v2 300 cycle, Illumina) with the first 15 cycles of read 1 set to dark cycling and using custom primers 22 and 23 (**Table S7**). The PhiX amount was set to 10%.

Finally the polyA site was introduced back into the vector separating the barcode from the regulatory sequence using the *BamH*I and *KpnI* restriction sites that were introduced in the oligo design. We digested the PolyA Minus library with *Kpn*I (NEB, 37°C o.n.), followed by gel purification and digestion with *BamHI* in the presence of Shrimp Phosphatase (NEB) for 2h at 37°C. In parallel, we digested overnight 20 ugr of the pGEMT-polyA vector to release the SV40 polyA signal (230 bp) with *KpnI* and *BamHI* and gel purified it. We cleaned both fragments with Agencourt AMPure beads and quantified them using Qubit 1X dsDNA BR Assay Kit (ThermoFisher). For each bin we used 100 ngr of the input vector and a 2:1 insert:vector ratio in the T4 ligase 16°C overnight reactions. We purified the ligations with Agencourt AMPure beads and performed electroporations in the same conditions as the ones used for the PolyA Minus library. After evaluating the efficiency of the electroporation we seeded 0.5 million cfu per 245 mm Square BioAssayDish with Agar+Ampicillin, keeping at least 100 CFU per oligo element. A step-by-step protocol of the procedure is available in protocols.io[50].

MPRA Nucleofection and parallel mRNA and gDNA isolation

Cells were seeded at 1.5 to 2x10^5 /ml into 2-4 T175 flasks (Corning, CLS431085-50EA) in 60 ml

of fresh medium (9 to 12 million cells each flask), and cultured for 48 hours changing half of their media 24 hours after seeding. The electroporation was performed using the Neon Transfection System (ThermoFisher). In K-562 and HL-60 we electroporated 5 million cells with 25 ugr of a pool of the three plasmid bins per reaction (12.5 ugr of the Medium GC bin and 6.25 ugr of each of the other two bins). In the case of CHRF-288-11 and THP-1 cells we electroporated 5 million cells with a four plasmid mix (10 ugr of the Medium GC bin, 5 ugr of each of the other two bins and 5 ugr of the pMAX-GFP vector). The nucleofection was performed following the manufacturer instructions using buffer R. The conditions for K-562, THP-1 and CHRF-288-11 cells were 1.45 v, 10 ms pulse width and 3 pulses, for HL60 1.350 v, 35 ms pulse width and 1 pulse.The efficiency of the nucleofection was evaluated at 24h and 48h post nucleofection in the pmaxGFP plate with a Countess II FL Automated Cell Counter. We routinely observed 80-90% efficiency for K-562 cells. In the case of CHRF-288-11 and THP-1 due to the low transfection efficiency cells were co-transfected with pMAX-GFP and we used FACS to purify GFP positive cells as a way to enrich cells that have incorporated plasmids in the nucleofection step.

48 h post-electroporation cells were spun down (300G 5') and resuspended in DNase I (NEB) at 37□ for 15' using 10 U of enzyme per ug of plasmid transfected in a final volume of 2 ml of DPBS to eliminate possible carryover plasmid in the exterior of the cells. Cells were then pelleted (300 G for 5'), washed twice with DPBS and lysed in 600 ul of Buffer RLT Plus (Qiagen) with added β-mercaptoethanol and homogenised using QIAshredder columns (Qiagen 79654). DNA and total RNA were extracted using AllPrep DNA/RNA Kit (Qiagen) according to the manufacturer's instructions. In the RNA preparation, a step of on-column DNase I treatment was performed for all samples (Rnase_Free Dnase Set, Qiagen). We isolated mRNA from total RNA using the Oligotex mRNA Kit (Qiagen) followed by a final treatment with Turbo Dnase (Invitrogen). DNA and mRNA quantifications were done using Qubit RNA Quantification, high sensitivity assay (ThermoFisher) . A detailed protocol can be found in[51,52].

MPRA Library preparation and sequencing

We retrotranscribed 1-1,5 ug of mRNA per replica following the protocol for SuperScript IV (ThermoFisher) using a reporter specific RT primer (Primer 24, **Table S7**) at 2uM carrying the 10-mer UMIs. Then we split retrotranscription samples for PCR amplification so as the RT template would represent 10% of the final volume of the PCR (50 ul). We performed the first round of amplification in which we introduced the sample index primer, i5-i8 (Primers 15-18 **Table S7**) for the cDNA samples of four replicas. As a reverse primer, we used P7 (Primer 21 **Table S7**). The PCR was carried out using Kapa HiFi HS Ready Mix, and 65□ annealing temperature for a total of 3 cycles. The amplification from each replica was then pooled, purified using Agencourt AMPure XP beads and then we assessed the minimum number of cycles for a second round of PCR by q-PCR with P5 and P7 with StepOnePlus™ Real-Time PCR System (ThermoFisher, Primers 20 and 21 **Table S7**). We determined between 11 and 13 cycles to be a good average range to keep the second round PCR from plateauing. Following Klein et al[24] we split each of the replicas into 8 reactions and performed the second round PCR for the cycles determined with the P5 and P7 primers and Kapa HiFi HS Ready Mix at 64□ annealing temperature. We then pooled the reactions from each replica, purified using Agencourt AMPure XP beads and eluted in 60

ul of Elution Buffer.

The gDNA fraction from the All Prep Qiagen kit was used as a source for the episomal plasmid nucleofected in every replica. For every replica, we used 12 ugr of gDNA that was split into 24 PCR reactions following Klein et al[24]. In this first reaction we introduced the sample index and the UMIs using the primers 11-14 (**Table S7**) as forward primers and primer 24 (**Table S7**) as reverse primer. The PCR was run for 3 cycles at 65□ annealing temperature and the reactions corresponding to each replica were pooled, purified using Agencourt AMPure XPbeads and eluted in 320 ul of Elution Buffer. As in the cDNA library preparation we assessed by qPCR the number of cycles to keep the second round PCR from plateauing. We determined 10-11 cycles. We split each of the replicas into 29 reactions and performed the second round PCR with the P5 and P7 primers and Kapa HiFi HS Ready Mix at 72°C annealing temperature. Finally, we pooled the reactions for each replica, purified 200 ul of the mix using Agencourt AMPure XP system (1.2X vol/vol of beads) and eluted in 30 ul of Elution Buffer.

All the libraries were quantified using KAPA Illumina SYBR Universal Lib Q. Kit, adjusted to 4nM and pooled afterwards in 40 ul final volume. We used a HiSeq 2500 RR for sequencing each batch with the Hiseq Rapid PE Cluster Kit V2 (Illumina) and the HiSeq Rapid SBS Kit v2 200 cycles (Illumina FC-402-4021). The recipe included the first 15 cycles of read 1 set to dark cycling and used custom primers 22, 25 and 26 from **Table S7**. The amount of PhiX was set to 10%. A detailed protocol can be found in[52].

MPRA alignments and count matrix

The first six nucleotides of the r2 reads corresponding to the *BamHI* site (see protocols io) were removed. UMIs were added to each read ID in r1 and r2 files using UMI tools[53] and merged using flash[54] prior to aligning against the reference set of barcodes using bwa[55]. Only primary alignments were taken forward. We discarded alignments not matching perfectly the corresponding barcodes with bamtools[56] and deduplicated the UMIs per barcode using UMI tools. Finally we counted all the unique UMIs across all the tagging barcodes of a regulatory sequence.The pipeline is available in GitHub[57].

INTERVAL WGS analysis workflow

The INTERVAL whole genome sequencing data (WGS) were generated at the Wellcome Sanger Institute. The manuscript describing WGS in full is in preparation. Briefly, WGS was performed on 12,354 samples using the Illumina HiSeq X10 platform as paired-end 151 bp reads. Raw read processing was carried out via customised pipelines at WSI. Reads were aligned with BWA MEM to the GRCh38 human reference genome with decoys (also known as HS38DH). Variants were called for each sample using GATK HaplotypeCaller version 4.0.0. Then all samples were merged, and the combined samples genotyped using GATK4.0.10.1. GATK Variant Quality Score Recalibration (VQSR) was used to identify probable false positive calls by assigning quality score log-odds (VQSLOD) separately for SNPs and INDELs using GATK VariantRecalibrator (v4.0.10.1). Sample quality control removed 491 samples in total, including 77 samples with coverage below 12x, 134 samples with > 3% non-reference discordance (NRD), 118 samples with > 3% FreeMix (VerifyBamID2) score, 221 samples failing identity checks, 30 samples swapped, 40 samples failing sex checks, 39 duplicates and 9 samples with possible contamination. Genotypes with allele read balance > 0.1 for homozygous reference variants, <

0.9 for homozygous alternative variants or not between 0.2-0.8 for heterozygous variants were removed. Genotypes were also removed if the proportion of informative reads was < 0.9 or read depth > 100. We performed additional variant quality control and filtered out variants that failed to meet the following requirements: call rate per site > 95%, mean genotype quality (GQ) value > 20, Hardy-Weinberg equilibrium (HWE) p-value > 1 x 10^{-6} only for autosomes. All monomorphic variants with alternative allele count (AAC) = 0 were further removed, although we kept all monomorphic variants with reference allele count (RAC) = 0. For chrX and chrY we applied an additional step to correct allele counts and frequencies due to female and male samples accounting for diploidy/haploidy in the PAR and non-PAR regions. Finally, the WGS data set contains 116,382,870 variants (100,694,832 SNVs and 15,688,038 indels) including 6,637,420 (5.7%) multi-allelic sites across 11,863 participants.

INTERVAL RNA-Seq analysis workflow

The INTERVAL RNA-sequencing data were generated and processed as previously described[30]. We mapped the RNA-sequencing data to the GRCh38 reference and quantified read counts as described previously[58] with the difference of using GENCODE v31 across 4,731 samples passing quality control. Globin genes, rRNA genes, and pseudogenes were removed. 19,841 genes were selected with > 0.5 CPM in at least 1% of the samples. Gene expression counts were converted to FPKM, trimmed mean of M-values (TMM) normalised and $\log_2$ transformed. We used the probabilistic estimation of expression residuals (PEER) method[59], implemented in the R package peer v.1.0[60], to correct for latent batch effects and other unknown confounders. 50 PEER factors were calculated with age, sex, BMI, and 19 blood cell traits included as covariates.

For transcript quantification we used Salmon v1.1.0[61]. The Salmon index was built against GRCh38 cDNA. R packages tximport v1.14.2, AnnotationHub v2.18.0, BiocFileCache v1.10.2, BiocGenerics v0.32.0 were applied to obtain various count matrices from these quantifications at the transcript or gene level. We subsetted to 4,731 samples passing RNA sequencing QC and corrected sample swaps. We focused on the transcripts of the 19,841 genes that passed gene QC. From these transcripts, we selected transcripts with TPM ≥ 0.1 in at least 20% samples. Subsequently, TPM values were TMM normalised and log2 transformed.

GTEx and INTERVAL sQTLs

For the 20 genes with ATU in our survey of INTERVAL whole blood RNA-seq (*ATL1, NPRL3, VMP1, ELP5, KDSR, RASAL3, SLC11A1, MFSD2B, GATA2, EEFSEC, TAF8, IKZF1, PILRB, ANK1, GFI1B, EVI5, TYMP, ARSA, ODF3B* and *PILRB*) we queried the GTEx[32] web portal (release v8) and found sQTLs in whole blood for *PILRB, SLC11A1, ARSA, ANK1, MFSD2B, TAF8, GFI1B* and *RASAL3*. The same query in the INTERVAL web[62] yielded 16 genes: *MFSD2B, PILRB, TYMP, ANK1, ARSA, EVI5, NPRL3, VMP1, GFI1B, SLC11A1, IKZF1, EEFSEC, ODF3B, TAF8 GATA2* and *RASAL3*. We obtained all the proxy variants at R^2=0.7 in the European subpopulations (EUR) in a window size of 0.5 Mb for all the sQTLs in these genes using LDLinkR[63]. None of the index variants leading to ATU were proxies of the GTEx sQTLs. Three of the index variants with ATU genes (rs149489081-*ANK1*, rs543594419-*TYMP, ODF3B* and *ARSA* and rs187715179-*GFI1B*) were sQTLs in the same genes in INTERVAL. The code for this analysis is available in GitHub[64,65].

Predicting TF motifs intersecting rs139141690 A > G

For the 94 variants screened in MPRA we selected a sequence stretch of 38 bp centred on the SNP and extracted the reference allele sequence. In the case of the 80-bp deletion we used the complete 80 bp nucleotide stretch. We then substituted the reference allele with the alternative allele in the position of the SNP to obtain the alternative allele version. We predicted TF motifs in both the reference and alternative allele versions of the 38 bp nucleotide stretch with gimme motifs[66] with the reference databases HOMER[67] and JASPAR[68], the -c option set to 0.85 and the maximum number of TF motif per nucleotide stretch set to 20. To assess TF occupancy we intersected the motifs with CHIP-seq data from whole blood present in the CHIP atlas database[69]. In the case of variant rs139141690 the occupancy of the PU.1 motif in the reference genome is supported by CHIP-seq data of PU.1 in 121 experiments in whole blood (ids: ERX626856, ERX626869, SRX093183, SRX093189, SRX100429, SRX100443, SRX100576, SRX10144602, SRX10144603, SRX1023790, SRX1023791, SRX1023792, SRX1023793, SRX103224, SRX1048461, SRX1089832, SRX1089833, SRX1127545, SRX12684447, SRX12684451, SRX1431740, SRX14869351, SRX14869352, SRX14869358, SRX14869359, SRX18154277, SRX18154278, SRX18154279, SRX18154280, SRX190299, SRX19553539, SRX20230007, SRX20230008, SRX20230009, SRX2268282, SRX2268283, SRX2268284, SRX2268285, SRX2268286, SRX2268287, SRX24542848, SRX24542849, SRX2770854, SRX2770855, SRX2770856, SRX2770857, SRX3824041, SRX3824042, SRX4001818, SRX4001819, SRX4001820, SRX4001821, SRX4001958, SRX4001959, SRX4001960, SRX4001961, SRX4484984, SRX475793, SRX475794, SRX5141098, SRX5141099, SRX5574342, SRX5574343, SRX5574345, SRX5574346, SRX5574348, SRX5574350, SRX5574352, SRX5574354, SRX5574355, SRX5574356, SRX5574357, SRX5574359, SRX5574361, SRX5574362, SRX5574363, SRX5574364, SRX5574365, SRX5574367, SRX5574369, SRX5574370, SRX5574373, SRX5574375, SRX5574376, SRX5574379, SRX5574381, SRX5574385, SRX5574387, SRX5574392, SRX5574446, SRX5574447, SRX5574448, SRX5574449, SRX5574450, SRX5574451, SRX5574452, SRX5574453, SRX5574457, SRX5574458, SRX5574459, SRX5574460, SRX5574461, SRX5574462, SRX5574463, SRX5574491, SRX5574492, SRX5574493, SRX5574494, SRX5574498, SRX5574499, SRX5574500, SRX5574505, SRX5574506, SRX5574507, SRX627428, SRX627430, SRX698188, SRX698189, SRX794057, SRX9029196, SRX9029197, SRX9029208, SRX9029209). The FOXM1 motif is supported by whole blood CHIP-seq data in 1 experiment (id: SRX190187) . The scripts are available on GitHub[70].

GenIE CRISPR/Cas9 targeting and amplicon design

We followed the protocol described in Cooper et al[12]. The Wellcome Sanger Institute Genome Editing browser (WGE)[71], was used to choose CRISPR gRNAs with NGG PAM site within 20bp of the SNP locus and with less than 1-3 mismatch off-target hits predicted. To introduce the SNP of interest a 100bp repair template oligonucleotide was designed. As a positive control for cutting we used the sgRNA against ENSG00000178927/ CYBC1/ EROS (numbers 39-43 from **Table S7**).

Primers were designed to amplify <250bp across the SNP of interest, 40-60% GC, Tm 56-65°C (NEB Tm Calculator) and with adaptor sequence tails for MiSeq Sequencing (See **Table S7**). Reverse transcriptase primers were designed downstream of the amplicon in the mRNA sequence (See **Table S7**).

GenIE Nucleofection

Guide RNAs (IDT) were annealed to tracrRNA (IDT) in duplex buffer (IDT 1072570) at 95°C for 2 min and cooled slowly to RT. Nucleofection on Kolf2_c1 was carried out as previously described[72] and recovered onto 4ng/ul Synthemax-II (Corning CLS3535) coated 6 well plates. K-562 and HL-60 were nucleofected following Lonza's protocols. THP1 were nucleofected following Lonza's primary monocyte protocol. Cells were cultured for 1-2 weeks until confluent and snap frozen as 2-3 $x10^6$ cell pellets.

GenIE Library preparation and sequencing

Genomic DNA was extracted using DNA MagAttract HMW extraction kit (Qiagen), following standard instructions and eluted in 100ul H20. Total RNA was extracted using Direct-zol RNA Miniprep Plus kit (Zymo), TURBO DNAse treated and run on a 2100 RNA Nano Chip in a Bioanalyser (Agilent). Gene specific RT primers were annealed using 2ug RNA, 2uM RT primer and 10mM dNTPs, heated to 65°C for 5 min and placed on ice. cDNA synthesis was setup using half the annealed RNA, Superscript IV and RNasin (Promega) on ice and heated 50°C 10min, 55°C 10min, 60°C 10 min, 80°C 10min, 4°C hold.

Genomic DNA and whole RNA were amplified with PowerUP SYBR green master mix (Applied Biosystems A25742) or Q5 Hot Start polymerase (NEB), 10uM adaptor sequence primers with 4 PCR replicates for gDNA and 8 PCR replicates for cDNA. PCR conditions for PowerUP SYBR reactions were as previously described[12]. PCR conditions for Q5 Amplicons: 98°C 30s, (98°C 10s, 57°C 20s, 72°C 20s)x30, 72°C 2min. Amplicons were barcoded using WTSI PCR barcoding primers, pooled, gel extracted using Minelute kit (Qiagen 28604) and quantified by qPCR (KAPA library quantification). The prepared library was loaded onto a MiSeq System (Illumina) at 4nM with 20% PhiX using MiSeq Reagent Kit v2 300 cycles.

Generation of clone lines: CRISPR/Cas9 sgRNA designs and protocol

To introduce the rs139141690 (G>A) mutation into K-562 cells, a synthetic crRNA was selected using CRISPOR[73] (**Table S7,** number 46). An 81bp ssODN carrying the mutation G>A was chemically made by IDT with 4 phosphorothioate bonds (**Table S7,** number 47). To delete the 80 bp region encompassing the rs139141690 two crRNAs were selected one upstream and one downstream of the desired SNP (**Table S7,** 48-49).

The crRNA and trans-activating crRNA (tracrRNA) were synthesised by IDT. An electroporation enhancer was also bought by IDT and resuspended at 100 µM in water. SgRNAs are made by combining 160 µM of crRNA and tracrRNA (1:1 v/v) to get a final concentration of 80 µM and incubated at 37C for 30 min.

To assemble the Cas9/sgRNA RNPs, the sgRNAs and electroporation enhancer (0.8:1 volume ratio) were first mixed and then 40µM S.p. Cas9 Nuclease (IDT) at 1:1 v/v was added. This mixture was incubated at 37C for 15-30 min prior use.

Electroporation was performed using SF Cell Line 4D-Nucleofector™ X Kit (Lonza) according to manufacturer's instructions. The kit / program for K-562 used is SF kit / FF-120.

For the *knock-in* experiment, 50 pmol *of the RNP* was electroporated into K-562 cells together with 4µM ssODN as HDR template. 15 min after electroporation cells are incubated with a combination of 0.5µM Trichostatin A (TSA, Selleckem) and 1µM M3814 (Selleckem) to enhance the HDR as previously reported in Shy et al[74]. 24 hours post treatment drugs are removed and fresh medium is added[74]. For the deletion of 80 bp, 50 pmol of each of the two RNPs was electroporated.

After 24h cells were single-cell sorted in 96 wells plates using MoFlo Astrios (Beckman Coulter). Propidium Iodide (Sigma Aldrich) was added prior to analysis as a cell viability dye.

Generation of clone lines: isolation of clones and genotyping by amplicon sequencing

K-562 clones were let to grow from single cells for 10-14 days, then genomic DNA was extracted with the QIAamp 96 DNA QIAcube HT Kit and quantified using the QuantiFluor® dsDNA System (Promega). 2-5 ng of DNA from every colony were used as template for targeted amplicon sequencing (**Table S7**, 44-45). Samples were then indexed with Nextera XT DNA Library Preparation Kit (Illumina), pooled and sequenced on NovaSeq 6000 (Illumina, 500 cycles, PE). Data were analysed by using CRISPResso2 v2.2.12[75] and clones with the desired genotypes were expanded to generate the modified cell lines.

In the same nucleofection we isolated: i) three clone lines homozygous reference for the SNP rs139141690 chr7:101499930 ('G/G'), ii) one heterozygous clone line chr7:101499930 ('A/G') and iii) three homozygous alternative clone lines chr7:101499930 ('A/A'). In addition to this we isolated: i) one homozygous clone line carrying the deletion of 16 bp (chr7:101499917 CTCACTAGAGCAAGTCC > C) and ii) three homozygous clone lines carrying the 80 bp deletion (chr7:101499894 GTTAGTGACTTCAAAAGCTGTCCTCACTAGAGCAAGTCCAACTCTTCCTCTA GTTCTGATGACTTCACGGCAGCCAACTG > G). All the coordinates are in GRCh37.

Generation of clone lines: lentiviral barcoding

Plasmids carrying single unique barcodes were isolated from the Larry Barcode Library V1[76] (Addgene, #140025) characterised by whole plasmid sequencing (Eurofins) to identify the different barcodes and used to transfect Phoenix Ampho (ATCC, CRL-3213) cells, together with the pMD2.G[77] (Addgene, #12259) and psPAX2[77] (Addgene, #12260) lentiviral packaging vectors. 48h after the transfection, the viral supernatant was collected, filtered, and used to infect the K-562 clones with the different genotypes, in presence of 6ug/ml polybrene.
GFP+ cells were sorted after 4 days and expanded to obtain 11 different cell lines (K-562-Larry), each one carrying a specific barcode, detectable both at gDNA and mRNA level.

Flow cytometry tracking of CD41 expressing K-562 cells

K-562 cells were seeded at 100.000 cells/ml in IMDM + 10% FBS and cultured in presence of 5nM phorbol 12-myristate 13-acetate (PMA, Selleckchem) or DMSO for 16, 24, 48 and 72 hours. For each time point cells were analysed by flow cytometry and collected for RNA extraction.
For flow cytometry tracking, cells were washed in PBS and incubated with anti-CD235a BUV395 (Clone GA-R2, BD Biosciences) and anti-CD41 AF700 (clone HIP8, Biolegend) antibodies for 20 min at 4°C in PBS + 1% FCS + 2mM EDTA. Cells were then washed and acquired with the CytoFLEX (Beckman Coulter) flow cytometer. DAPI (Sigma Aldrich) was added prior to analysis as a cell viability dye. Data was analysed using the FlowJo software.

10X Multiome nuclei isolation

For each time point, cells were analysed by flow cytometry and 50.000 cells per genotype were pooled for nuclei isolation. Single nuclei were isolated using the Nuclei Prep Buffer (Zymo Research), counted and processed following the Chromium Single Cell Multiome ATAC + Gene Expression workflow[78].

10X Multiome aligning and QC

10x genomics multiome data were processed using Cell Ranger ARC (2.0.2) using default parameters and the provided reference genome GRCh38-2020-A-2.0.0. Initial filtering steps were applied to the raw gene expression and peak (ATAC) matrices of each sample using functions from the Seurat and Signac (v5) packages[79,80]. Cells with <500 gene features were first removed and the package scDBfinder[81] was used to mark doublets in both RNA and ATAC data. Further, cells with < 1000 peak features, >10% mitochondrial reads, and multiplets marked by cellranger were removed. At this stage, doublets were additionally identified in the ATAC data using Amulet[82]. Prior to merging samples, ATAC matrices were rebuilt to reflect unique fragment counts in 5kb genomic windows instead of peaks, using a custom pipeline[83], and RNA matrices were adjusted to remove ambient contamination using CellBender[84]. The merged Seurat object

was then filtered to retain cells that could be unequivocally assigned to a lentiviral Larry barcode. To deconvolute samples based on the lentiviral barcodes, reads that did not map to the reference genome were extracted from the original cellranger genome + transcriptome alignments (gex_possorted_bam.bam) using samtools view -f 4, converted to fastq, and then re-mapped to a new reference containing the 11 possible GFP+barcodes transgenes. Multimappers were then removed (samtools view -q 5) to keep only the reads uniquely mapping to each GFP barcode. For each read, molecular barcode (UMI), cell barcode and Larry barcode were recorded. Only cell/Larry barcodes combinations supported by a minimum of 3 UMI were retained. Cell barcodes were assigned to a genotype only if one cell/Larry barcodes combination was found. The RNA and ATAC reductions from the merged and filtered Seurat object were then integrated using the Weighted Nearest Neighbour (WNN) analysis following the steps and recommended parameters in guidelines[85]. For clustering analysis on the integrated WNN graph, the Leiden algorithm with resolution 2 was used. At this stage, a low-quality cluster with lower read counts and higher mitochondrial content was removed, as well as doublets, which were previously marked as such by both Amulet and scDBfinder. After these final filters, we called ATAC peaks on the remaining cells with MACS2 (2.2.9.1) using the Signac callPeaks function and generated a new feature ATAC matrix with these peak coordinates, which replaced the window matrix. WNN analysis was then repeated as above, but with 0.5 resolution for the final clusters. The final object was composed of 13 clusters, 11.250 cells, ~29.000 genes and ~357.000 peaks. Processing and analysis codes can be found in Github[86].

Quantification and statistical analysis

Comparisons between sets of variants

In the case of the comparison with pathogenic variants, the list was obtained from Table 1 Vuckovic et al[2] and restricted to GWAS traits associated with the pathogenic variants. Index variants had higher effect sizes to reported heterozygous blood ClinVar/HGMD pathogenic variants[2] (median absolute effect size values 0.169 and 0.13 respectively, p value = 0.009, *Wilcoxon test*)

For the comparisons shown in **Figure 1C** we used pairwise Wilcoxon tests to assess statistically significant differences between categories, applying multiple testing correction (Benjamini–Hochberg) across all the comparisons. The scripts are in GitHub[87]. Median values of MAF: Tier 1 0.285, Tier 2 0.013, Tier 3 0.018, Tier 4 0.016 and index variants 0.007.
Median values of PPFM: Tier 1 0.01, Tier 2 0.422, Tier 3 0.012, Tier 4 0.986 and index variants 0.999. Median values of absolute effect size: Tier 1 0.019, Tier 2 0.092, Tier 3 0.062, Tier 4 0.075 and index variants 0.152. Median values of CADD raw: Tier 1 -0.009, Tier 2 1.189, Tier 3 -0.049, Tier 4 0.034 and index variants 0.119. Median values of Gnocchi: Tier 1 0.653, Tier 2 1.834, Tier 3 0.868, Tier 4 1.203 and index variants 1.235. Median values of NCBoost: Tier 1 0.029, Tier 2 0.076, Tier 3 0.031, Tier 4 0.045 and index variants 0.077.

Conditional analysis of common variants on the index variants

To condition for known common variants associated with the studied traits, we run GWAS of 29 blood cell counts in ~409 UK Biobank individuals of white British ancestry, following the procedure described in[1], the scripts are available in GitHub[88]. Accordingly, we employed the same phenotype exclusions, adjustments and normalisation approach, and ran GWAS using REGENIE[89] and TOPMed imputed genotypes[90], including recruitment center and the first ten PCs of the kinship matrix as covariates. We then obtained independently associated variants for

each trait by using the GCTA (v1.94.1) cojo[91] joint model function (with parameters: collinearity = 0.9, p-value < 1e-4) and LD structure estimates from the genotypes of 30,000 unrelated individuals of white British ancestry from UK Biobank samples. Finally, for each of the 123 rare variants, we gathered all independent GWAS common variants obtained by cojo, having MAF > 1% and joint association p-value < $1x10^{-7}$, and falling within a +/- 500kb window from a rare variant. We then performed conditional analysis by fitting a linear regression model of the blood trait and the genotype of the associated rare variant, including the genotypes of the independent GWAS hits as covariates. The model was fitted in R (using the stats::lm function) and genotypes of both common and rare variants were obtained from the WGS of UK Biobank 200k release (GraphTyper population level WGS variants, PLINK format). Out of 123 rare non-coding variants, genotypes were available for 80 of them; of these 80, 76 (95%), were significantly (p-value < 0.05) associated with at least one blood trait even after jointly conditioning for common variants.

MPRA analysis

We used MPRAmodel[25] to estimate enhancer activity (measured as log2 Fold Change, log2FC) and allelic specific expression (measured as log2 Allelic Skew, log2AS) per each tile, index variant and cell type. First we generated the necessary input files for MPRAmodel per cell type: a count matrix with the oligos and the barcodes in the rows and the columns (countsData), a file detailing the replicate breakdown between cDNA and gDNA libraries (condData) and an attributes files detailing each of the oligos attributes (attributesData). In the majority of the cases the tiles carried only one SNP so the 'Allele' field of the attributes table was set to ref or alt. For the 8 cases of diplotypes (two SNPs present in the same tile) we carried out all the possible comparisons and set the 'Allele' field of the attributes table to ref ref vs alt ref, ref ref vs ref alt and ref ref vs alt alt according to the tiles analysed. Next we adapted the MPRAmodel Rscript[92] from the MPRASuite to run the dataOut function on our inputs. The results were collected per cell type and tile and are shown in **Table S3**. We then performed a meta-analysis for each variant across all the tiles assayed to come up with a single value of activity per variant and cell type following[10,93]. The results of the meta-analysis are shown in **Table S4**. To establish the log2FC threshold that defines enhancer activity we employed a set of variants previously described to have MPRA activity in K-562 cells[9] as well as four regions deprived of CRISPRa activity in the same cell line[23](**Supplementary Figure 1A**). We considered active variants those with a log2FC higher than 0.25 at 1% global false-discovery rate (gFDR) (68 variants) and we additionally required that the log2AS was significant at 10% gFDR to label variants as MPRA positive (43 variants). Positive and negative Log2FC values indicate enhancer and repressor activity, respectively. Positive log2AS values correspond to a skew of the enhancer activity towards the alternative allele and negative values towards the reference allele. The analysis scripts are in GitHub[94].

MPRA lasso regression on annotated features

Enformer values[29] were obtained from the vcf file of the 94 variants screened in the MPRA and cell matched features were selected for K-562 cells (455 features) and HL-60 cells (6 features). GWAS parameters, orthogonal scores and cell-matched Enformer features were combined in a unique matrix per variant to perform lasso regression on the continuous variable log2FC. We performed the lasso regression for ten iterations and selected predictive variables that had coefficients greater than 0 in at least three. Positive coefficients indicate that higher values of the sequence feature are predictive of higher values of Log2FC. Conversely, negative coefficients indicate that higher values of the sequence feature are predictive of lower values of Log2FC.

In the case of the lasso regression for predictive variables of a qualitative variable, first we transformed the labels into integers (MPRA negative RNA+ = 0 and Double positive = 1) and then we ran the lasso regression with all the features and selected those that had coefficients greater than 0 in at least one iteration. Positive coefficients indicated that higher values of the sequence feature are predictive of the double-positive class. Conversely, negative coefficients indicate that higher values of the sequence feature are predictive of belonging to the MPRA-/RNA+ class. The expression values for the K-562 genes in the basal state were obtained from ENCODE[42]. The analysis scripts are in GitHub[95].

INTERVAL Differential Expression linear model

We modelled FPKM normalised raw values for each gene with a linear model using as covariates the PEER factors (top 35 from 50), top 10 genotype principal components, sex, age, BMI, RIN, sequencing batch, RNA concentration, read depth, and season (based on month of blood draw). Depending on the blood phenotypes associated with the variants at PP >= 0.1 we included a set of cell-count specific covariates (see **Table S1**) to account for cell count effects on total blood composition.

For each variant, we tested a median of 12 genes by combining all expressed genes within the GWAS association blocks (median size of 0.5 Mb) and those connected with index variants through PCHi-C interactions[46]. The multiple testing correction was done using the Benjamini–Hochberg method at three levels for each variant: i) all transcripts of all the genes in which the variant had a direct VEP Most Severe Consequence (LOF, MISS, SYN, UTR5, UTR3, INTRON, SPLICE, UPSTREAM), ii) all transcripts of all the genes within the GWAS association block plus the genes connected to the variant via PCHi-C (Block and PCHiC levels) and iii) Only for variants in Table 1, all the transcripts of all the genes (genome wide). The code used in this analysis is in GitHub[96].

INTERVAL Alternative Transcript Usage (ATU) additive logratio model

We calculated the median transcript ratio (median transcript TPM/median Expression of the gene to which the transcript belongs) for homozygous reference and heterozygous carriers separately. We discarded all transcripts with median transcript ratios below 0.1 in both genotypes to filter out transcripts whose contribution to the total expression of a given gene remains low irrespective of the genotype.

Given the compositional nature of the data we decided to transform proportions using the additive logratio model. Briefly, for all of the transcripts belonging to the same gene we first estimated the transcript ratio of gene expression (expression of the transcript/sum of the expression of all the transcripts belonging to the same gene) and scaled it to a reference transcript. The most abundant transcript was chosen as the reference transcript for each gene to avoid having 0 values at the denominator. This proportion was then log transformed. To avoid having transcripts with 0 TPM value in the logratio model, for any given transcript we imputed the value of the samples with 0 TPM to 0.65 of the minimum value greater than 0 for that transcript as this value is suggested to limit the distortion of the covariance matrix[97]. The resulting log scaled ratio per transcript was used in a linear regression model with the same constitutive and cell count specific covariates (see **Table S1**) per variant as the ones used in the DE model.

The multiple testing correction of the ATU model was done using the Benjamini–Hochberg

method at two levels for each variant: i) all transcripts of all the genes in which the variant had a direct VEP Most Severe Consequence (LOF, MISS, SYN, UTR5, UTR3, INTRON, SPLICE, UPSTREAM), ii) all transcripts of all the genes within the GWAS association block plus the genes connected to the variant via PCHi-C (Block and PCHi-C levels).The code used in this analysis is in GitHub[96]. To represent the transcripts we used ggtranscript[98].

BluePrint Differential Expression linear model

We used the normalised gene quantification - values from BLUEPRINT data [3]. We then applied a linear model to the gene quantification values for each gene.

The multiple testing correction was done using the Benjamini–Hochberg method at two levels for each variant: i) all transcripts of all the genes in which the variant had a direct VEP Most Severe Consequence (LOF, MISS, SYN, UTR5, UTR3, INTRON, SPLICE, UPSTREAM) and ii) all transcripts of all the genes within the GWAS association block plus the genes connected to the variant via PCHi-C (Block and PCHiC levels).

The code used in this analysis is in GitHub[99].

BluePrint Alternative Transcript Usage (ATU) additive logratio model

We calculated the median transcript ratio (median transcript FPKM/median Expression of the gene to which the transcript belongs) for homozygous reference and heterozygous carriers per cell type separately. For every cell type of BLUEPRINT we discarded all transcripts with median transcript ratios below 0.1 in both genotypes.

The same compositional model and multiple testing correction used for whole blood was applied in the BLUEPRINT per cell type. The code used in this analysis is in GitHub[99].

INTERVAL GSEA and ORA

For the GSEA analysis we started from the 22 variants in **Table 1** and performed a genome wide DE analysis between carriers and non-carriers per variant in the INTERVAL whole blood dataset. Next, we used the Fold Change between WT and HET genotypes to order the genes in a decreasing manner and input the ordered gene list into the GSEA function of ClusterProfiler[100]. The minimum and maximum gene set size and the p value cutoff were set to 10, 500 and 0.05, respectively. The multiple testing was accounted for by Benjamini & Hochberg. The code used in this analysis is in GitHub[96].

For the ORA analysis we started by defining a list of gene sets for blood and immunity from the Molecular Signatures Database (MSigDB)[101]: we first selected all the gene sets that contained in their description at least one of the following blood and immunity related terms: PLATELET, ERYTHRO, MEGAKARYOCYTE, MONOCYTE, NEUTROPHIL, EOSINOPHIL, BASOPHIL, LYMPHOCYTE, T_HELPER, TH_17, TH17, TH1, TH2, BLOOD, BLOOD_COAGULATION, IMMUNE, HUMORAL_IMMUNE_RESPONSE, IMMUNOGLOBULIN and HEMATOPOIETIC. We also included two blood and immunity unrelated terms (HEPATOCYTE and NEURON). In addition, we included in the ORA analysis TF target gene sets for the TFs *GATA2, GFI1, CUX1* and *RUNX1* in the Dorothea collection[102] (A,B ,C and D confidence levels). The minimum and maximum gene set size allowed was 10 and 500, respectively, but for the Dorothea gene sets which were exempted from this filter (*CUX1* n=464 genes, *FOXP1* n=3,278, *GATA2* n=5,370, *GFI1* n=8 and *RUNX1*

n=2,551). The list of selected pathways (*n=1,423 gene sets*) can be found in GitHub[103]. Next, we tested the genome wide DE analysis of the 22 variants in **Table 1** used for the GSEA for overrepresentation of DE genes applying Active Pathways[104] with the significant p value cutoff set to 0.01. As a background list of gene sets we used all the gene sets derived from the Human Phenotype ontology (c5.hpo.v2023.2.Hs.entrez.gmt, *n=5,547 gene sets*[39,101]). We obtained 64 pathways significantly overrepresented in DE genes of which 3 were from the unrelated terms. The remaining 65 pathways corresponded to 11 variants. We excluded from further analysis the gene sets from Dorothea (2 variants). A variant was labelled as 'ORA positive' if it had at least 1 ORA pathway at p value = 0.05. To test if the 9 variants were enriched in the TF annotation (**Table 1**) we used a Chi square test (6/7 variants with TF annotation vs 3/15 non TF labelled variants were 'ORA positive', p value = 0.0141). The code is located in GitHub[103].

Comparison of number of carriers between variants with DE/ATU regulation and variants without effect in the RNA-seq studies

Median number of heterozygous carriers for variants with DE and/or ATU = 43 and median number of heterozygous carriers for variants without RNA-seq effect = 36, p value = 0.045, *Wilcoxon test*.

GenIE analysis

Read pairs per amplicon were merged using flash[54] with the following parameters: read length (-r) 150, fragment sd (-s) 20, minimum overlap (-m) 10. Fragment size (-f) and maximum mismatch density (-x) depended on the targeted amplification: CUX1 (223, 0.115) and ENSG00000178927/CYBC1/EROS (249, 0.12). The reads were aligned using bwa mem[105] with the following parameters: -O 24,48 -E 1 -A 4 -B 16 -T 70 -k 19 -w 200 -d 600 -L 20 -U 40. The aligned reads were filtered to discard reads with more than 10 clipped bases using samclip[106]. The GenIE results were obtained using the rgenie package[12,107] allowing for 10 bases for the required_match_right and required_match_left parameters. The scripts are available in GitHub[37].

Flow cytometry data ILR compositional analysis

We collected the percentages of $CD41^{-}CD235^{-}$, $CD41^{-}CD235^{+}$, $CD41^{+}CD235^{+}$, $CD41^{+}CD235^{-}$ cells and the value of CD41 MFI and GeoMFI at the four time points of the PMA differentiations per genotype and clone line (*n=3* clone lines per genotype). The 'Basal' time point was assigned to cells mock treated for 16 hours. We used the package Compositions[108,109] to transform the cell abundance percentages into isometric log ratios (ilr)[110]. Next we model the ILR values using as covariates time (reduced model) and time and Genotype (full model) and tested the significance between adding the different terms to the models by ANOVA. The code for the analysis is located in GitHub[111].

Cell size using flow cytometry FSC-A and SSC-A

We collected the values of FSC-A and SSC-A per cell, genotype and time point and restricted our analysis to $CD41^{+}CD235^{-}$ cells at 72 hours as they were the most mature cell type in our model (*n=4,892, 8,914* and *7,553* for the wild type clone lines, *n=3,616, 4,307* and *6,229* for the homozygous alternative clone lines and *n=9,822, 6,476* and *9,611* for the 80 bp deletion clone lines). The median values for FSC-A are: 585312 (G/G genotype), 592815 (A/A genotype) and 647251 (Del80 genotype). The median values for SSC-A are: 391532 (G/G genotype), 407041 (A/A genotype) and 468646 (Del80 genotype). We used the Wilcoxon-rank test to analyse

differences between the cells. The code is located in GitHub[112].

10X Multiome DE and DA analysis

The code and the detailed list of dependencies can be found in GitHub[113]. Briefly, for the DE analysis we aggregated the counts of all the cells belonging to the same combination of clone line, time point and Seurat cluster using the function Seurat2PB (Seurat v5.01[79]). Then, per Seurat cluster, we used DESeq2[114] to calculate a linear model accounting for time (reduced model) or for time and genotype (complete model) and applied a Likelihood ratio test (LRT) to test cases in which the complete model was a significantly better fit to the data following analysis guidelines for time and condition differential analysis[115,116].

For the ORA analysis we started by defining a list of gene sets relevant for K-562 differentiation from the Molecular Signatures Database (MSigDB)[101]: we selected all the gene sets that contained in their description at least one of the following terms: PLATELET, ERYTHROCYTE, CUX1, MEGAKARYOCYTE, GATA1, GATA2, TET2, RUNX1, RUNX2, MITOSIS, ANEUPLOIDY, CYTOKINESIS, MYELOID, AML, LIPID, SPHINGOSINE, FOXM1, SPI1, PU1, PI3K, AKT, FOXP1 and GFI1. We also included two blood and immunity unrelated terms (HEPATOCYTE and NEURON). In addition, we included in the ORA analysis TF target gene sets for the TFs *GATA2, GFI1, CUX1* and *RUNX1* in the Dorothea collection[102] (A,B ,C and D confidence levels). The minimum and maximum gene set size allowed was 10 and 500, respectively, but for the Dorothea gene sets which were exempted from this filter (*CUX1* n=464 target genes, *FOXP1* n=3,278, *GATA2* n=5,370, *GFI1* n=8 and *RUNX1* n=2,551). The list of selected pathways (*n=803 gene sets*) can be found in the GitHub repository. We obtained 59 pathways significantly overrepresented in DE genes of which 2 were from the unrelated terms.

For the DA analysis we first extracted all the linked peaks to the set of DE genes and a set of marker genes (in total 1,897 genes) using the LinkPeaks function of Signac (v1.12.0)[80]. To characterise the linked peaks (n=14,211 peaks) we overlapped them with annotated gene TSS (+/- 2.5 kB of the TSS, n= 4,072 overlaps with a known TSS, ENSEMBL, release 111[117]) and with the annotated regulatory features of the basal state K-562 cells (ENSEMBL, release 111[118]). Next, we produced a reduced seurat object with the ATAC counts of the selected peaks using the function CreateChromatinAssay (Signac v1.12.0) and then obtained a new Seurat object with the assay option set to 'RNA' as the function Seurat2PB (Seurat v5.01) would not work if it was set to 'ATAC'. From this point onwards the pipeline proceeded as explained in the DE analysis. To clusterize the results of both analyses we used Pheatmap[119] and to display them in volcano plots and in detailed locus plots we used ggplot2[120].

Additional resources

MPRA library synthesis and cloning protocol:
https://www.protocols.io/edit/mpra-synthesis-library-design-and-cloning-soranzo-cs3awgie

Step by step protocol used to design and clone the MPRA oligos into the reporter vector.

MPRA nucleofection: https://www.protocols.io/edit/mpra-synthesis-cellular-work-and-nucleofection-sor-cs3jwgkn

Step by step protocol used to nucleofect the library into the cancer cell lines.

MPRA library preparation for sequencing: https://www.protocols.io/edit/mpra-synthesis-dna-rna-isolation-and-library-prepa-cs3mwgk6

Step by step protocol used to extract and prepare the different MPRA libraries for sequencing.

Haemvar architecture/ documentation: https://haemvar.org

We created the HaemVar Database of genetic variants and blood-related traits, containing the complete association and fine-mapping result data set of all the variants associations to 29 blood cell phenotypes assessed by Vuckovic et al[2], and including further annotation data for the prioritised subset of 178,890 variants as described above; see section 'Variant Annotation'. All information contained in the HaemVar Database is presented through an open-access website that generates comprehensive gene and variant-specific data reports with downloadable tables and figures. The software of the web-based application is written in PHP for server-side handling and optimisation of database access and data output, and uses the open-source Vega v5 (http://vega.github.io) JavaScript library for custom generation of data-driven and (partially) interactive visualisations.

Declaration of generative AI and AI-assisted technologies in the writing process

During the preparation of this work the author(s) used ChatGPT in order to improve language and readability. After using this tool/service, the author(s) reviewed and edited the content as needed and take(s) full responsibility for the content of the publication.

References

1. Astle, W.J., Elding, H., Jiang, T., Allen, D., Ruklisa, D., Mann, A.L., Mead, D., Bouman, H., Riveros-Mckay, F., Kostadima, M.A., et al. (2016). The Allelic Landscape of Human Blood Cell Trait Variation and Links to Common Complex Disease. Cell *167*, 1415–1429.e19.

2. Vuckovic, D., Bao, E.L., Akbari, P., Lareau, C.A., Mousas, A., Jiang, T., Chen, M.-H., Raffield, L.M., Tardaguila, M., Huffman, J.E., et al. (2020). The Polygenic and Monogenic Basis of Blood Traits and Diseases. Cell *182*, 1214–1231.e11.

3. Chen, L., Ge, B., Casale, F.P., Vasquez, L., Kwan, T., Garrido-Martín, D., Watt, S., Yan, Y., Kundu, K., Ecker, S., et al. (2016). Genetic Drivers of Epigenetic and Transcriptional Variation in Human Immune Cells. Cell *167*, 1398–1414.e24.

4. Võsa, U., Claringbould, A., Westra, H.-J., Bonder, M.J., Deelen, P., Zeng, B., Kirsten, H., Saha, A., Kreuzhuber, R., Yazar, S., et al. (2021). Large-scale cis- and trans-eQTL analyses identify thousands of genetic loci and polygenic scores that regulate blood gene expression. Nat. Genet. *53*, 1300–1310.

5. Kundu, K., Tardaguila, M., Mann, A.L., Watt, S., Ponstingl, H., Vasquez, L., Von Schiller, D., Morrell, N.W., Stegle, O., Pastinen, T., et al. (2022). Genetic associations at regulatory phenotypes improve fine-mapping of causal variants for 12 immune-mediated diseases. Nat. Genet. *54*, 251–262.

6. Parums, D.V. (2024). Editorial: First regulatory approvals for CRISPR-Cas9 therapeutic gene editing for sickle cell disease and transfusion-dependent β-thalassemia. Med. Sci. Monit. *30*, e944204.

7. Uda, M., Galanello, R., Sanna, S., Lettre, G., Sankaran, V.G., Chen, W., Usala, G., Busonero, F., Maschio, A., Albai, G., et al. (2008). Genome-wide association study shows BCL11A associated with persistent fetal hemoglobin and amelioration of the phenotype of beta-thalassemia. Proc. Natl. Acad. Sci. U. S. A. *105*, 1620–1625.

8. Frangoul, H., Altshuler, D., Cappellini, M.D., Chen, Y.-S., Domm, J., Eustace, B.K., Foell, J., de la Fuente, J., Grupp, S., Handgretinger, R., et al. (2021). CRISPR-Cas9 gene editing for sickle cell disease and β-thalassemia. N. Engl. J. Med. *384*, 252–260.

9. Ulirsch, J.C., Nandakumar, S.K., Wang, L., Giani, F.C., Zhang, X., Rogov, P., Melnikov, A., McDonel, P., Do, R., Mikkelsen, T.S., et al. (2016). Systematic Functional Dissection of Common Genetic Variation Affecting Red Blood Cell Traits. Cell *165*, 1530–1545.

10. Siraj, L., Castro, R.I., Dewey, H., Kales, S., Nguyen, T.T.L., Kanai, M., Berenzy, D., Mouri, K., Wang, Q., McCaw, Z.R., et al. (2024). Functional dissection of complex and molecular trait variants at single nucleotide resolution. bioRxiv. https://doi.org/10.1101/2024.05.05.592437.

11. Sample, P.J., Wang, B., Reid, D.W., Presnyak, V., McFadyen, I.J., Morris, D.R., and Seelig, G. (2019). Human 5' UTR design and variant effect prediction from a massively parallel translation assay. Nat. Biotechnol. *37*, 803–809.

12. Cooper, S.E., Schwartzentruber, J., Bello, E., Coomber, E.L., and Bassett, A.R. (2020). Screening for functional transcriptional and splicing regulatory variants with GenIE. Nucleic Acids Res. *48*, e131.

13. Morris, J.A., Caragine, C., Daniloski, Z., Domingo, J., Barry, T., Lu, L., Davis, K., Ziosi, M., Glinos, D.A., Hao, S., et al. (2023). Discovery of target genes and pathways at GWAS loci by pooled single-cell CRISPR screens. Science, eadh7699.

14. Turro, E., Astle, W.J., Megy, K., Gräf, S., Greene, D., Shamardina, O., Allen, H.L., Sanchis-Juan, A., Frontini, M., Thys, C., et al. (2020). Whole-genome sequencing of patients with rare diseases in a national health system. Nature *583*, 96–102.

15. Muerdter, F., Boryń, Ł.M., Woodfin, A.R., Neumayr, C., Rath, M., Zabidi, M.A., Pagani, M., Haberle, V., Kazmar, T., Catarino, R.R., et al. (2018). Resolving systematic errors in widely used enhancer activity assays in human cells. Nat. Methods *15*, 141–149.

16. Yao, D., Tycko, J., Oh, J.W., Bounds, L.R., Gosai, S.J., Lataniotis, L., Mackay-Smith, A., Doughty, B.R., Gabdank, I., Schmidt, H., et al. (2024). Multicenter integrated analysis of noncoding CRISPRi screens. Nat. Methods *21*, 723–734.

17. Martin-Rufino, J.D., Castano, N., Pang, M., Grody, E.I., Joubran, S., Caulier, A., Wahlster, L., Li, T., Qiu, X., Riera-Escandell, A.M., et al. (2023). Massively parallel base editing to map variant effects in human hematopoiesis. Cell. https://doi.org/10.1016/j.cell.2023.03.035.

18. Ribeiro, D.M., and Delaneau, O. (2023). Non-coding rare variant associations with blood traits on 166 740 UK Biobank genomes. bioRxiv, 2023.12.01.569422. https://doi.org/10.1101/2023.12.01.569422.

19. Rentzsch, P., Witten, D., Cooper, G.M., Shendure, J., and Kircher, M. (2019). CADD: predicting the deleteriousness of variants throughout the human genome. Nucleic Acids

Res. *47*, D886–D894.

20. Caron, B., Luo, Y., and Rausell, A. (2019). NCBoost classifies pathogenic non-coding variants in Mendelian diseases through supervised learning on purifying selection signals in humans. Genome Biol. *20*. https://doi.org/10.1186/s13059-019-1634-2.

21. Chen, S., Francioli, L.C., Goodrich, J.K., Collins, R.L., Kanai, M., Wang, Q., Alföldi, J., Watts, N.A., Vittal, C., Gauthier, L.D., et al. (2023). A genomic mutational constraint map using variation in 76,156 human genomes. Nature. https://doi.org/10.1038/s41586-023-06045-0.

22. Melnikov, A., Murugan, A., Zhang, X., Tesileanu, T., Wang, L., Rogov, P., Feizi, S., Gnirke, A., Callan, C.G., Jr, Kinney, J.B., et al. (2012). Systematic dissection and optimization of inducible enhancers in human cells using a massively parallel reporter assay. Nat. Biotechnol. *30*, 271–277.

23. Fulco, C.P., Munschauer, M., Anyoha, R., Munson, G., Grossman, S.R., Perez, E.M., Kane, M., Cleary, B., Lander, E.S., and Engreitz, J.M. (2016). Systematic mapping of functional enhancer–promoter connections with CRISPR interference. Science *354*, 769–773.

24. Klein, J.C., Agarwal, V., Inoue, F., Keith, A., Martin, B., Kircher, M., Ahituv, N., and Shendure, J. (2020). A systematic evaluation of the design and context dependencies of massively parallel reporter assays. Nat. Methods. https://doi.org/10.1038/s41592-020-0965-y.

25. Tewhey, R., Kotliar, D., Park, D.S., Liu, B., Winnicki, S., Reilly, S.K., Andersen, K.G., Mikkelsen, T.S., Lander, E.S., Schaffner, S.F., et al. (2016). Direct identification of hundreds of expression-modulating variants using a multiplexed reporter assay. Cell. https://doi.org/10.1016/j.cell.2016.04.027.

26. Maeß, M.B., Wittig, B., and Lorkowski, S. (2014). Highly efficient transfection of human THP-1 macrophages by nucleofection. J. Vis. Exp., e51960.

27. K-562 Cellosaurus. https://web.expasy.org/cellosaurus/CVCL_0004.

28. HL-60 Cellosaurus. https://web.expasy.org/cellosaurus/CVCL_0002.

29. Avsec, Ž., Agarwal, V., Visentin, D., Ledsam, J.R., Grabska-Barwinska, A., Taylor, K.R., Assael, Y., Jumper, J., Kohli, P., and Kelley, D.R. (2021). Effective gene expression prediction from sequence by integrating long-range interactions. Nat. Methods *18*, 1196–1203.

30. Tokolyi, A., Persyn, E., Nath, A.P., Burnham, K.L., Marten, J., Vanderstichele, T., Tardaguila, M., Stacey, D., Farr, B., Iyer, V., et al. (2025). The contribution of genetic determinants of blood gene expression and splicing to molecular phenotypes and health outcomes. Nat. Genet. https://doi.org/10.1038/s41588-025-02096-3.

31. Love, M.I., Soneson, C., and Patro, R. (2018). Swimming downstream: statistical analysis of differential transcript usage following Salmon quantification. F1000Res. *7*, 952.

32. Lonsdale, J., Thomas, J., Salvatore, M., Phillips, R., Lo, E., Shad, S., Hasz, R., Walters, G., Garcia, F., Young, N., et al. (2013). The genotype-tissue expression (GTEx) project. Nat. Genet. *45*, 580–585.

33. Polfus, L.M., Khajuria, R.K., Schick, U.M., Pankratz, N., Pazoki, R., Brody, J.A., Chen, M.-H., Auer, P.L., Floyd, J.S., Huang, J., et al. (2016). Whole-Exome Sequencing Identifies Loci Associated with Blood Cell Traits and Reveals a Role for Alternative GFI1B Splice Variants in Human Hematopoiesis. Am. J. Hum. Genet. *99*, 785.

34. Karczewski, K.J., Solomonson, M., Chao, K.R., Goodrich, J.K., Tiao, G., Lu, W., Riley-Gillis, B.M., Tsai, E.A., Kim, H.I., Zheng, X., et al. (2022). Systematic single-variant and gene-based association testing of thousands of phenotypes in 394,841 UK Biobank exomes. Cell Genomics *2*, 100168.

35. Mountjoy, E., Schmidt, E.M., Carmona, M., Schwartzentruber, J., Peat, G., Miranda, A., Fumis, L., Hayhurst, J., Buniello, A., Karim, M.A., et al. (2021). An open approach to systematically prioritize causal variants and genes at all published human GWAS trait-associated loci. Nat. Genet. *53*, 1527–1533.

36. An, N., Khan, S., Imgruet, M.K., Gurbuxani, S.K., Konecki, S.N., Burgess, M.R., and McNerney, M.E. (2018). Gene dosage effect of CUX1 in a murine model disrupts HSC homeostasis and controls the severity and mortality of MDS. Blood *131*, 2682–2697.

37. genIE_analysis https://github.com/manueltar/genIE_analysis/tree/main.

38. Mazzi, S., Dessen, P., Vieira, M., Dufour, V., Cambot, M., El Khoury, M., Antony-Debré, I., Arkoun, B., Basso-Valentina, F., BenAbdoulahab, S., et al. (2021). Dual role of EZH2 in megakaryocyte differentiation. Blood *138*, 1603–1614.

39. Gargano, M.A., Matentzoglu, N., Coleman, B., Addo-Lartey, E.B., Anagnostopoulos, A.V., Anderton, J., Avillach, P., Bagley, A.M., Bakštein, E., Balhoff, J.P., et al. (2024). The Human Phenotype Ontology in 2024: phenotypes around the world. Nucleic Acids Res. *52*, D1333–D1346.

40. Wong, C.C., Martincorena, I., Rust, A.G., Rashid, M., Alifrangis, C., Alexandrov, L.B., Tiffen, J.C., Kober, C., Chronic Myeloid Disorders Working Group of the International Cancer Genome Consortium, Green, A.R., et al. (2014). Inactivating CUX1 mutations promote tumorigenesis. Nat. Genet. *46*, 33–38.

41. Di Angelantonio, E., Thompson, S.G., Kaptoge, S., Moore, C., Walker, M., Armitage, J., Ouwehand, W.H., Roberts, D.J., Danesh, J., and INTERVAL Trial Group (2017). Efficiency and safety of varying the frequency of whole blood donation (INTERVAL): a randomised trial of 45 000 donors. Lancet *390*, 2360–2371.

42. ENCODE K-562 RNA report https://www.encodeproject.org/rnaget-report/?type=RNAExpression&file.assay_title=polyA+plus+RNA-seq&file.biosa\mple_ontology.classification=cell+line&file.biosample_ontology.term_name=K562&limit=all.

43. INTERVAL https://IntervalRNA.org.uk.

44. McLaren, W., Gil, L., Hunt, S.E., Riat, H.S., Ritchie, G.R.S., Thormann, A., Flicek, P., and Cunningham, F. (2016). The Ensembl Variant Effect Predictor. Genome Biol. *17*. https://doi.org/10.1186/s13059-016-0974-4.

45. VEP_most_severe https://www.ensembl.org/info/docs/tools/vep/script/vep_options.html.

46. Javierre, B.M., Sewitz, S., Cairns, J., Wingett, S.W., Várnai, C., Thiecke, M.J., Freire-Pritchett, P., Spivakov, M., Fraser, P., Burren, O.S., et al. (2016). Lineage-Specific Genome Architecture Links Enhancers and Non-coding Disease Variants to Target Gene Promoters. Cell *167*, 1369–1384.e19.

47. Ulirsch, J.C., Lareau, C.A., Bao, E.L., Ludwig, L.S., Guo, M.H., Benner, C., Satpathy, A.T., Kartha, V.K., Salem, R.M., Hirschhorn, J.N., et al. (2019). Interrogation of human hematopoiesis at single-cell and single-variant resolution. Nat. Genet. *51*, 683–693.

48. Lareau, C. ATAC data. https://github.com/caleblareau/singlecell_bloodtraits/tree/master/data/bulk/ATAC.

49. Arnold, C.D., Gerlach, D., Stelzer, C., Boryń, Ł.M., Rath, M., and Stark, A. (2013). Genome-wide quantitative enhancer activity maps identified by STARR-seq. Science *339*, 1074–1077.

50. MPRA synthesis Library design and cloning Soranzo Lab https://www.protocols.io/edit/mpra-synthesis-library-design-and-cloning-soranzo-cs3awgie.

51. MPRA synthesis Cellular work and Nucleofection Soranzo Lab https://www.protocols.io/edit/mpra-synthesis-cellular-work-and-nucleofection-sor-cs3jwgkn.

52. MPRA synthesis DNA/RNA isolation and library preparation for sequencing Soranzo Lab https://www.protocols.io/edit/mpra-synthesis-dna-rna-isolation-and-library-prepa-cs3mwgk6.

53. Smith, T., Heger, A., and Sudbery, I. (2017). UMI-tools: modeling sequencing errors in Unique Molecular Identifiers to improve quantification accuracy. Genome Res. *27*, 491–499.

54. Magoč, T., and Salzberg, S.L. (2011). FLASH: fast length adjustment of short reads to improve genome assemblies. Bioinformatics *27*, 2957–2963.

55. Li, H., and Durbin, R. (2009). Fast and accurate short read alignment with Burrows–Wheeler transform. Bioinformatics *25*, 1754–1760.

56. Barnett, D.W., Garrison, E.K., Quinlan, A.R., Strömberg, M.P., and Marth, G.T. (2011). BamTools: a C++ API and toolkit for analyzing and managing BAM files. Bioinformatics *27*, 1691–1692.

57. MPRA_bc_synthesis_Sample_alignment_and_counts https://github.com/manueltar/MPRA_bc_synthesis_Sample_alignment_and_counts.git.

58. Vanderstichele, T., Burnham, K.L., de Klein, N., Tardaguila, M., Howell, B., Walter, K., Kundu, K., Koeppel, J., Lee, W., Tokolyi, A., et al. (2023). Misexpression of inactive genes in whole blood is associated with nearby rare structural variants. bioRxiv, 2023.11.17.567537. https://doi.org/10.1101/2023.11.17.567537.

59. Stegle, O., Parts, L., Piipari, M., Winn, J., and Durbin, R. (2012). Using probabilistic estimation of expression residuals (PEER) to obtain increased power and interpretability of gene expression analyses. Nat. Protoc. *7*, 500–507.

60. Peer https://github.com/PMBio/peer.

61. Patro, R., Duggal, G., Love, M.I., Irizarry, R.A., and Kingsford, C. (2017). Salmon provides fast and bias-aware quantification of transcript expression. Nat. Methods *14*, 417–419.

62. INTERVAL web portal https://www.intervalrna.org.uk/.

63. Myers, T.A., Chanock, S.J., and Machiela, M.J. (2020). LDlinkR: An R Package for Rapidly Calculating Linkage Disequilibrium Statistics in Diverse Populations. Front. Genet. *11*, 157.

64. GTEx_sQTLs https://github.com/manueltar/GTEx_sQTLs/tree/main.

65. INTERVAL_sQTLs https://github.com/manueltar/INTERVAL_sQTLs.

66. van Heeringen, S.J., and Veenstra, G.J.C. (11 2010). GimmeMotifs: a de novo motif prediction pipeline for ChIP-sequencing experiments. Bioinformatics *27*, 270–271.

67. Heinz, S. et al (2010). Simple Combinations of Lineage-Determining Transcription Factors Prime cis-Regulatory Elements Required for Macrophage and B Cell Identities. Mol. Cell *38*, 576–589.

68. Castro-Mondragon, J.A., Riudavets-Puig, R., Rauluseviciute, I., Lemma, R.B., Turchi, L., Blanc-Mathieu, R., Lucas, J., Boddie, P., Khan, A., Manosalva Pérez, N., et al. (2022). JASPAR 2022: the 9th release of the open-access database of transcription factor binding profiles. Nucleic Acids Res. *50*, D165–D173.

69. Zou, Z., Ohta, T., Miura, F., and Oki, S. (2022). ChIP-Atlas 2021 update: a data-mining suite for exploring epigenomic landscapes by fully integrating ChIP-seq, ATAC-seq and Bisulfite-seq data. Nucleic Acids Res. *50*, W175–W182.

70. TF_motif_prediction_with_occupancy https://github.com/manueltar/TF_motif_prediction_with_occupancy.

71. Wellcome Sanger Institute Genome Editing browser (WGE) https://www.sanger.ac.uk/htgt/wge/.

72. Bruntraeger, M., Byrne, M., Long, K., and Bassett, A.R. (2019). Editing the Genome of Human Induced Pluripotent Stem Cells Using CRISPR/Cas9 Ribonucleoprotein Complexes. Methods Mol. Biol. *1961*, 153–183.

73. Concordet, J.-P., and Haeussler, M. (2018). CRISPOR: intuitive guide selection for CRISPR/Cas9 genome editing experiments and screens. Nucleic Acids Res. *46*, W242–W245.

74. Shy, B.R., Vykunta, V.S., Ha, A., Talbot, A., Roth, T.L., Nguyen, D.N., Pfeifer, W.G., Chen, Y.Y., Blaeschke, F., Shifrut, E., et al. (2022). High-yield genome engineering in primary cells using a hybrid ssDNA repair template and small-molecule cocktails. Nat. Biotechnol. https://doi.org/10.1038/s41587-022-01418-8.

75. Clement, K., Rees, H., Canver, M.C., Gehrke, J.M., Farouni, R., Hsu, J.Y., Cole, M.A., Liu, D.R., Joung, J.K., Bauer, D.E., et al. (2019). CRISPResso2 provides accurate and rapid genome editing sequence analysis. Nat. Biotechnol. *37*, 224–226.

76. Weinreb, C., Rodriguez-Fraticelli, A., Camargo, F.D., and Klein, A.M. (2020). Lineage tracing on transcriptional landscapes links state to fate during differentiation. Science *367*. https://doi.org/10.1126/science.aaw3381.

77. pMD2.G and psPAX2 https://www.addgene.org/12259/#how-to-cite.

78. single-cell-multiome-atac-plus-gene-expression https://www.10xgenomics.com/products/single-cell-multiome-atac-plus-gene-expression.

79. Hao, Y., Stuart, T., Kowalski, M.H., Choudhary, S., Hoffman, P., Hartman, A., Srivastava, A., Molla, G., Madad, S., Fernandez-Granda, C., et al. (2024). Dictionary learning for integrative, multimodal and scalable single-cell analysis. Nat. Biotechnol. *42*, 293–304.

80. Stuart, T., Srivastava, A., Madad, S., Lareau, C.A., and Satija, R. (2021). Single-cell chromatin state analysis with Signac. Nat. Methods *18*, 1333–1341.

81. Germain, P.-L., Lun, A., Garcia Meixide, C., Macnair, W., and Robinson, M.D. (2021). Doublet identification in single-cell sequencing data using scDblFinder. F1000Res. *10*, 979.

82. Thibodeau, A., Eroglu, A., McGinnis, C.S., Lawlor, N., Nehar-Belaid, D., Kursawe, R., Marches, R., Conrad, D.N., Kuchel, G.A., Gartner, Z.J., et al. (2021). AMULET: a novel read count-based method for effective multiplet detection from single nucleus ATAC-seq data. Genome Biol. *22*, 252.

83. Benaglio, P., Newsome, J., Han, J.Y., Chiou, J., Aylward, A., Corban, S., Miller, M., Okino, M.-L., Kaur, J., Preissl, S., et al. (2023). Mapping genetic effects on cell type-specific chromatin accessibility and annotating complex immune trait variants using single nucleus ATAC-seq in peripheral blood. PLoS Genet. *19*, e1010759.

84. Fleming, S.J., Chaffin, M.D., Arduini, A., Akkad, A.-D., Banks, E., Marioni, J.C., Philippakis, A.A., Ellinor, P.T., and Babadi, M. (2023). Unsupervised removal of systematic background noise from droplet-based single-cell experiments using CellBender. Nat. Methods *20*, 1323–1335.

85. weighted_nearest_neighbor_analysis https://satijalab.org/seurat/articles/weighted_nearest_neighbor_analysis.

86. Benaglio, P. Tardaguila_etal (Github).

87. Figure_1_comparisons_and_plots https://github.com/manueltar/Figure_1_comparisons_and_plots.

88. ukbiobank_fbc https://github.com/ariannalandini/ukbiobank_fbc/tree/master.

89. Mbatchou, J., Barnard, L., Backman, J., Marcketta, A., Kosmicki, J.A., Ziyatdinov, A., Benner, C., O'Dushlaine, C., Barber, M., Boutkov, B., et al. (2021). Computationally efficient whole-genome regression for quantitative and binary traits. Nat. Genet. *53*, 1097–1103.

90. Taliun, D., Harris, D.N., Kessler, M.D., Carlson, J., Szpiech, Z.A., Torres, R., Taliun, S.A.G., Corvelo, A., Gogarten, S.M., Kang, H.M., et al. (2021). Sequencing of 53,831 diverse genomes from the NHLBI TOPMed Program. Nature *590*, 290–299.

91. Yang, J., Ferreira, T., Morris, A.P., Medland, S.E., Genetic Investigation of ANthropometric Traits (GIANT) Consortium, DIAbetes Genetics Replication And Meta-analysis (DIAGRAM) Consortium, Madden, P.A.F., Heath, A.C., Martin, N.G., Montgomery, G.W., et al. (2012). Conditional and joint multiple-SNP analysis of GWAS summary statistics identifies additional variants influencing complex traits. Nat. Genet. *44*, 369–375, S1–S3.

92. MPRAmodel https://github.com/tewhey-lab/MPRASuite/blob/main/MPRAmodel/MPRAmodel.R#L31.

93. meta-analysis code https://github.com/julirsch/finemapped_mpra/blob/main/code/preprocess/mpra_meta.R.

94. MPRA_bc_synthesis_analysis_MPRAmodel https://github.com/manueltar/MPRA_bc_synthesis_analysis_MPRAmodel/tree/main.

95. lasso regression https://github.com/manueltar/lasso_regression/tree/main.

96. INTERVAL analysis code https://github.com/manueltar/INTERVAL_ANALYSIS.

97. Martín-Fernández, J.A., Barceló-Vidal, C., and Pawlowsky-Glahn, V. (2003). Dealing with Zeros and Missing Values in Compositional Data Sets Using Nonparametric Imputation. Math. Geol. *35*, 253–278.

98. Gustavsson, E.K., Zhang, D., Reynolds, R.H., Garcia-Ruiz, S., and Ryten, M. (2022). ggtranscript: an R package for the visualization and interpretation of transcript isoforms using ggplot2. Bioinformatics *38*, 3844–3846.

99. BluePrint Analysis https://github.com/manueltar/BluePrint_ANALYSIS.

100. Wu, T., Hu, E., Xu, S., Chen, M., Guo, P., Dai, Z., Feng, T., Zhou, L., Tang, W., Zhan, L., et al. (2021). clusterProfiler 4.0: A universal enrichment tool for interpreting omics data. Innovation (Camb) *2*, 100141.

101. Liberzon, A., Birger, C., Thorvaldsdóttir, H., Ghandi, M., Mesirov, J.P., and Tamayo, P. (2015). The Molecular Signatures Database (MSigDB) hallmark gene set collection. Cell Syst *1*, 417–425.

102. Garcia-Alonso, L., Holland, C.H., Ibrahim, M.M., Turei, D., and Saez-Rodriguez, J. (2019). Benchmark and integration of resources for the estimation of human transcription factor activities. Genome Res. *29*, 1363–1375.

103. Active_Pathways_ORA https://github.com/manueltar/Active_Pathways_ORA_with_Dorothea.

104. Paczkowska, M., Barenboim, J., Sintupisut, N., Fox, N.S., Zhu, H., Abd-Rabbo, D., Mee, M.W., Boutros, P.C., PCAWG Drivers and Functional Interpretation Working Group, Reimand, J., et al. (2020). Integrative pathway enrichment analysis of multivariate omics data. Nat. Commun. *11*, 735.

105. Li, H. (2013). Aligning sequence reads, clone sequences and assembly contigs with BWA-MEM. arXiv [q-bio.GN].

106. samclip https://github.com/tseemann/samclip.

107. rgenie https://github.com/Jeremy37/rgenie.

108. van den Boogaart, K.G., and Tolosana-Delgado, R. (2013). Analyzing Compositional Data with R (Springer Science & Business Media).

109. Compositions R package http://www.stat.boogaart.de/compositions/.

110. Egozcue, J.J., Pawlowsky-Glahn, V., Mateu-Figueras, G., and Barceló-Vidal, C. (2003). Isometric Logratio Transformations for Compositional Data Analysis. Math. Geol. *35*, 279–300.

111. ILR-compositional-analysis-of-Flow-cytometry-data https://github.com/manueltar/ILR-compositional-analysis-of-Flow-cytometry-data.

112. FSC_A_SSC_A_analysis https://github.com/manueltar/FSC_A_SSC_A_analysis/tree/main.

113. Multiome_downstream_analysis github. https://github.com/manueltar/Multiome_downstream_analysis/tree/main.

114. Love, M.I., Huber, W., and Anders, S. (2014). Moderated estimation of fold change and dispersion for RNA-seq data with DESeq2. Genome Biol. *15*, 550.

115. Single-cell RNA-seq: Pseudobulk differential expression analysis https://hbctraining.github.io/scRNA-seq_online/lessons/pseudobulk_DESeq2_scrnaseq.html.

116. Introduction to DGE - ARCHIVED https://hbctraining.github.io/DGE_workshop/lessons/08_DGE_LRT.html.

117. Harrison, P.W., Amode, M.R., Austine-Orimoloye, O., Azov, A.G., Barba, M., Barnes, I., Becker, A., Bennett, R., Berry, A., Bhai, J., et al. (2024). Ensembl 2024. Nucleic Acids Res. *52*, D891–D899.

118. RegulatoryFeatureActivity_K562 https://ftp.ensembl.org/pub/release-111/regulation/homo_sapiens/RegulatoryFeatureActivity/K562/.

119. Kolde, R., and Kolde, M.R. (2015). Package "pheatmap." R package *1*, 790.

120. Wickham, H. (2009). ggplot2: Elegant Graphics for Data Analysis (Springer Science & Business Media).

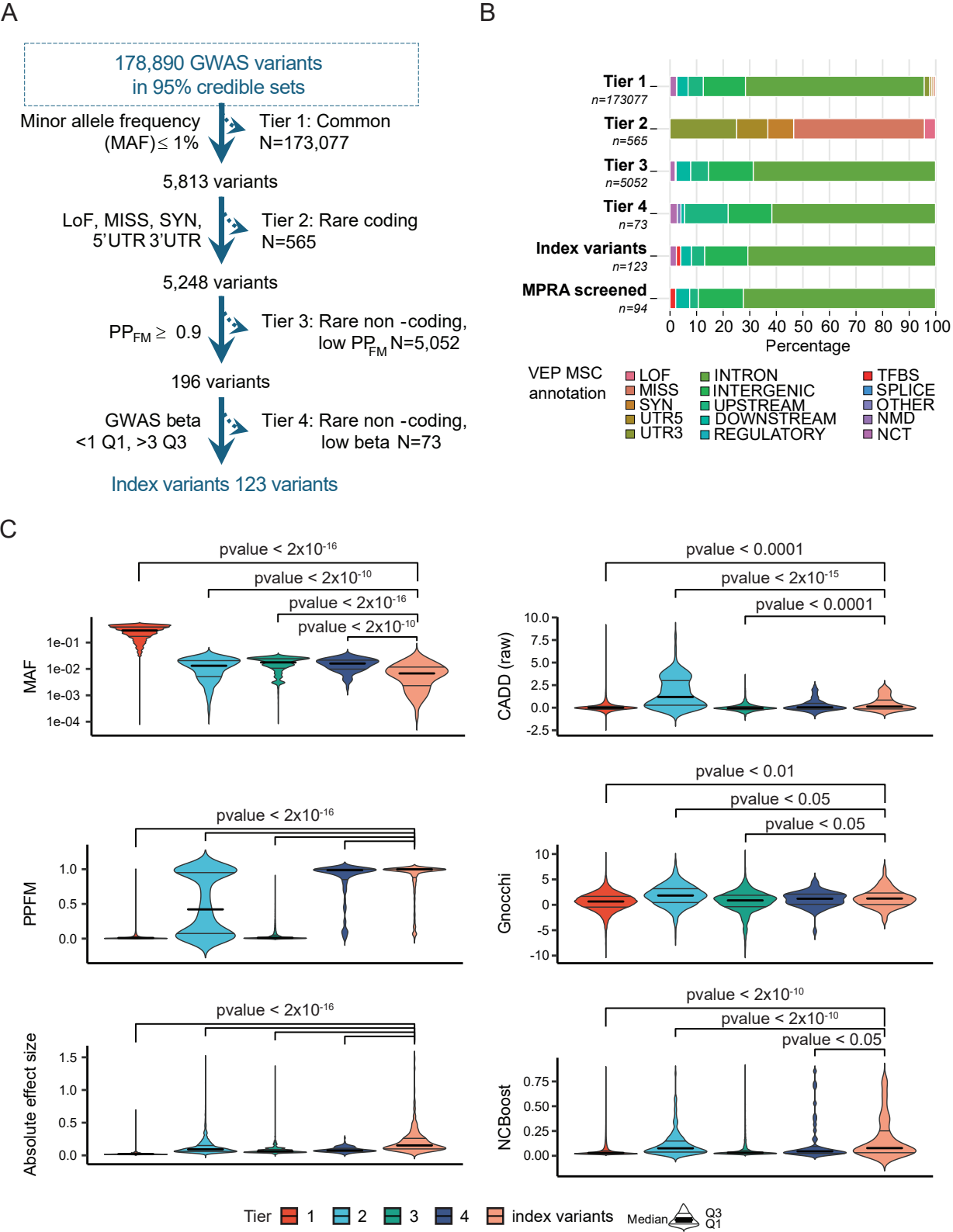
A
178,890 GWAS variants
in 95% credible sets
Minor allele frequency
(MAF)≤ 1%
Tier 1: Common
N=173,077
5,813 variants
LoF, MISS, SYN,
5'UTR 3'UTR
Tier 2: Rare coding
N=565
5,248 variants
PP_FM ≥ 0.9
Tier 3: Rare non -coding,
low PP_FM N=5,052
196 variants
GWAS beta
<1 Q1, >3 Q3
Tier 4: Rare non -coding,
low beta N=73
Index variants 123 variants
B
Tier 1 _ n=173077
Tier 2 _ n=565
Tier 3 _ n=5052
Tier 4 _ n=73
Index variants _ n=123
MPRA screened _ n=94
0 10 20 30 40 50 60 70 80 90 100
Percentage
VEP MSC annotation
LOF
MISS
SYN
UTR5
UTR3
INTRON
INTERGENIC
UPSTREAM
DOWNSTREAM
REGULATORY
TFBS
SPLICE
OTHER
NMD
NCT
C
MAF
pvalue < 2x10-16
pvalue < 2x10-10
pvalue < 2x10-16
pvalue < 2x10-10
1e-01
1e-02
1e-03
1e-04
CADD (raw)
pvalue < 0.0001
pvalue < 2x10-15
pvalue < 0.0001
10.0
7.5
5.0
2.5
0.0
-2.5
PPFM
pvalue < 2x10-16
1.0
0.5
0.0
Gnocchi
pvalue < 0.01
pvalue < 0.05
pvalue < 0.05
10
5
0
-5
-10
Absolute effect size
pvalue < 2x10-16
1.5
1.0
0.5
0.0
NCBoost
pvalue < 2x10-10
pvalue < 2x10-10
pvalue < 0.05
0.75
0.50
0.25
0.00
Tier 1 2 3 4 index variants
Median
Q3
Q1

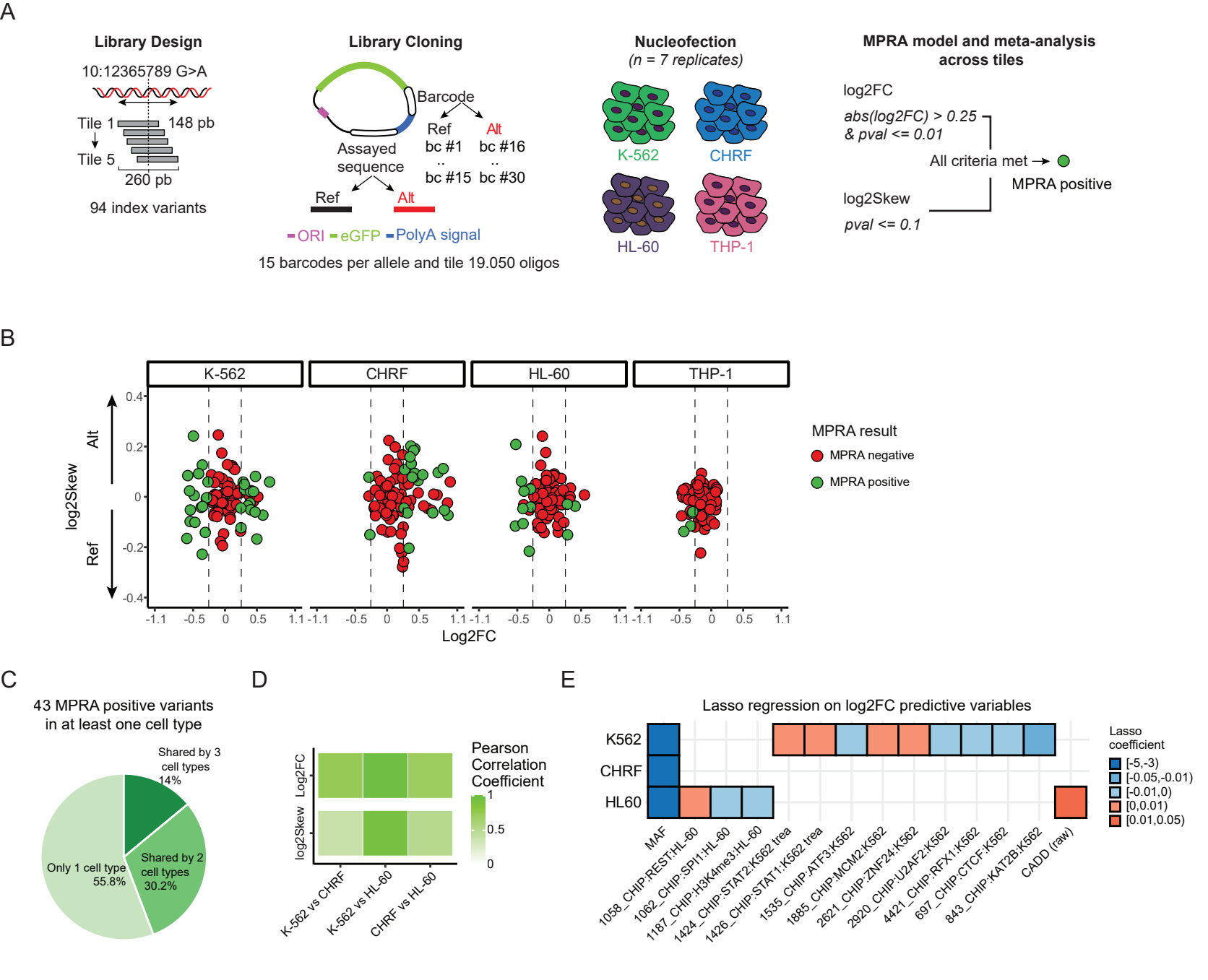
A
Library Design
10:12365789 G>A
Tile 1
148 pb
Tile 5
260 pb
94 index variants
Library Cloning
Barcode
Ref
Alt
bc #1
bc #15
bc #16
bc #30
Assayed sequence
Ref
Alt
ORI
eGFP
PolyA signal
15 barcodes per allele and tile 19.050 oligos
Nucleofection
(n = 7 replicates)
K-562
CHRF
HL-60
THP-1
MPRA model and meta-analysis across tiles
log2FC
abs(log2FC) > 0.25
& pval <= 0.01
All criteria met
MPRA positive
log2Skew
pval <= 0.1
B
K-562
CHRF
HL-60
THP-1
log2Skew
Alt
Ref
Log2FC
MPRA result
MPRA negative
MPRA positive
C
43 MPRA positive variants
in at least one cell type
Shared by 3 cell types 14%
Shared by 2 cell types 30.2%
Only 1 cell type 55.8%
D
Log2FC
log2Skew
Pearson Correlation Coefficient
K-562 vs CHRF
K-562 vs HL-60
CHRF vs HL-60
E
Lasso regression on log2FC predictive variables
K562
CHRF
HL60
Lasso coefficient
[-5,-3)
[-0.05,-0.01)
[-0.01,0)
[0,0.01)
[0.01,0.05)
MAF
1058_CHIP:REST:HL-60
1062_CHIP:SPI1:HL-60
1187_CHIP:H3K4me3:HL-60
1424_CHIP:STAT2:K562.trea
1426_CHIP:STAT1:K562.trea
1535_CHIP:ATF3:K562
1885_CHIP:MCM2:K562
2621_CHIP:ZNF24:K562
2920_CHIP:U2AF2:K562
4421_CHIP:RFX1:K562
697_CHIP:CTCF:K562
843_CHIP:KAT2B:K562
CADD (raw)

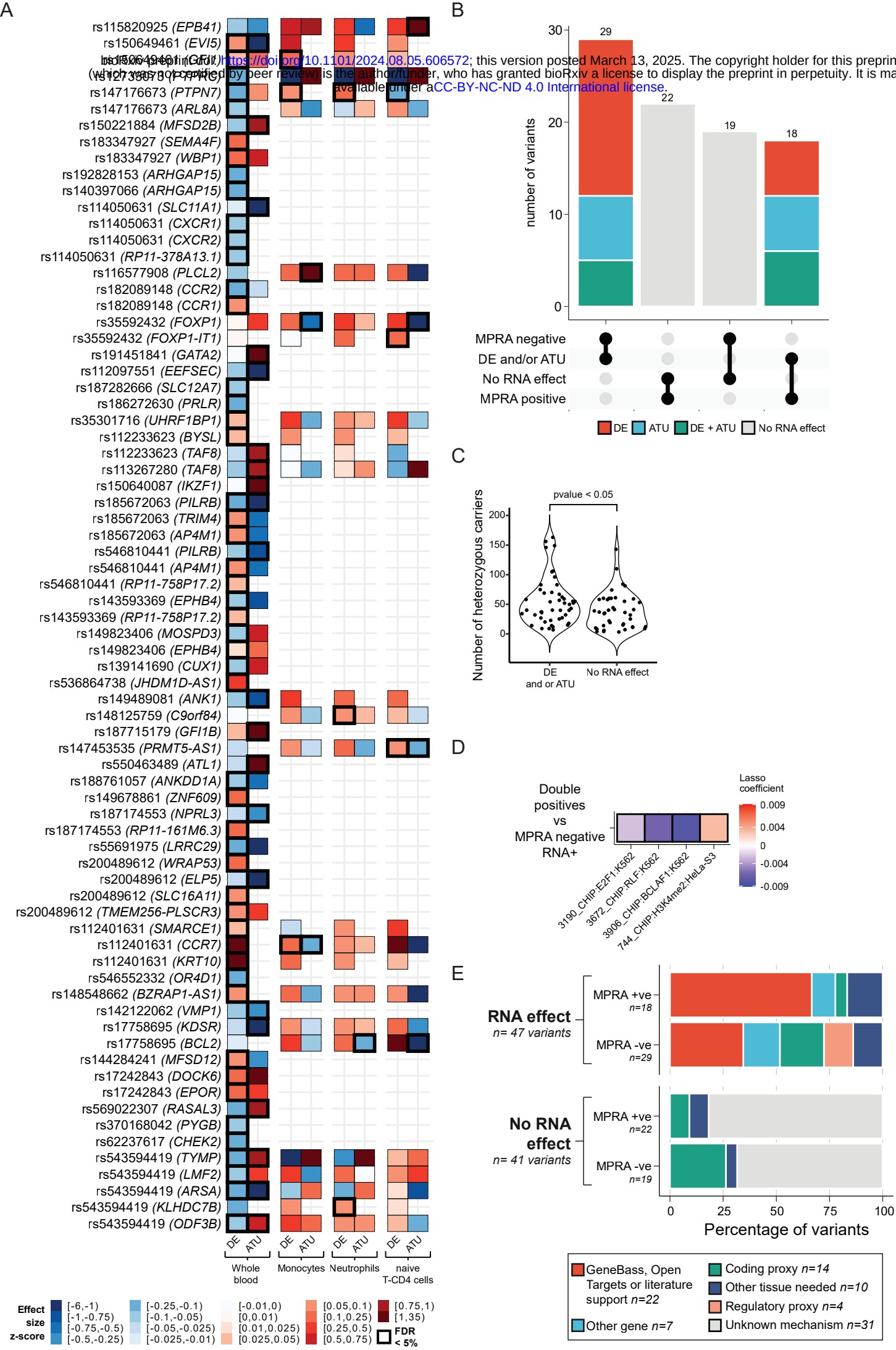

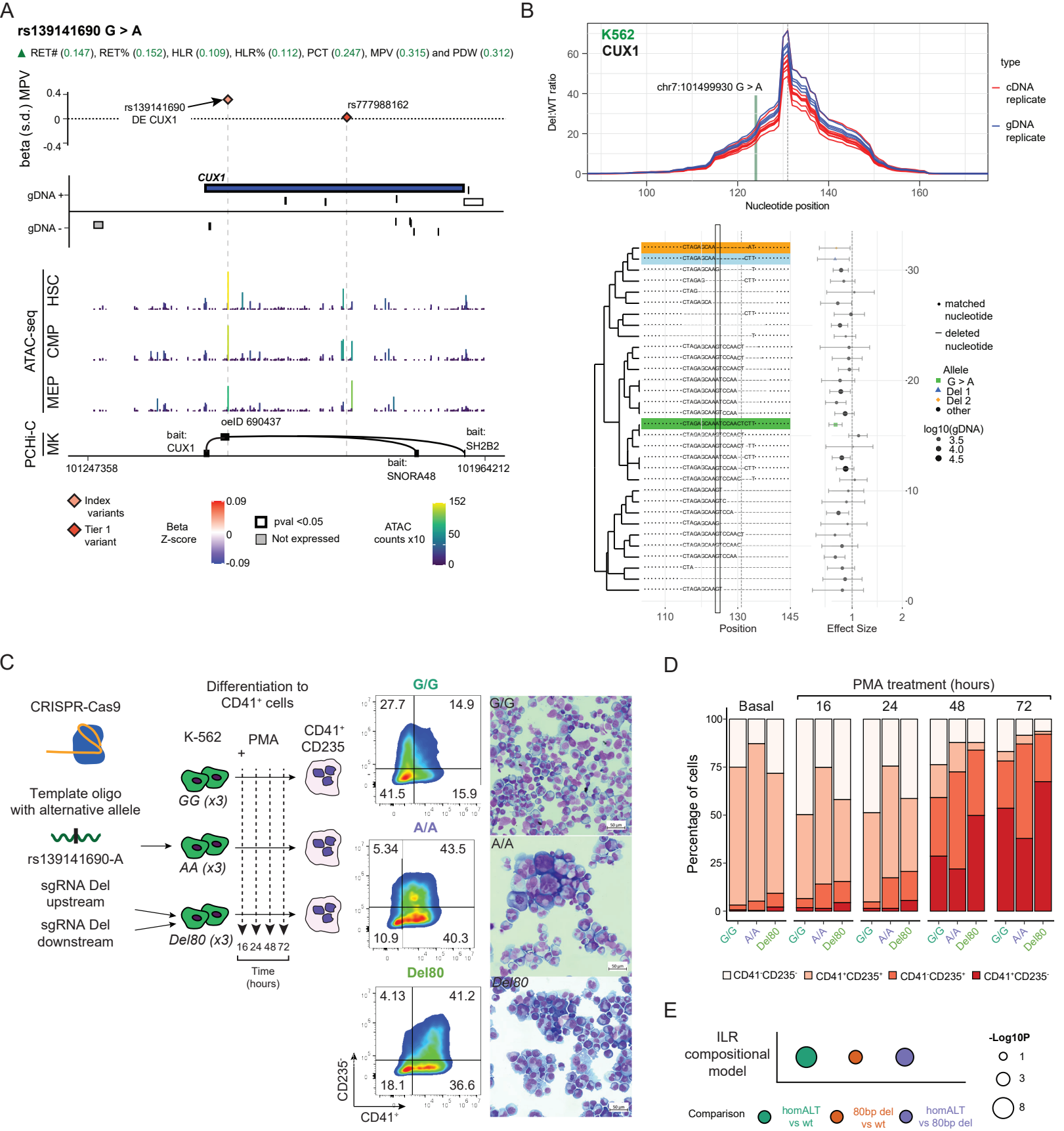
A
rs139141690 G > A
RET# (0.147), RET% (0.152), HLR (0.109), HLR% (0.112), PCT (0.247), MPV (0.315) and PDW (0.312)
beta (s.d.) MPV
rs139141690
DE CUX1
rs777988162
CUX1
gDNA +
gDNA -
ATAC-seq
HSC
CMP
MEP
PCHi-C
MK
oeID 690437
bait: CUX1
bait: SH2B2
bait: SNORA48
101247358
101964212
Index variants
Tier 1 variant
Beta Z-score
pval <0.05
Not expressed
ATAC counts x10
B
K562
CUX1
chr7:101499930 G > A
Del:WT ratio
Nucleotide position
type
cDNA replicate
gDNA replicate
Position
Effect Size
matched nucleotide
deleted nucleotide
Allele
G > A
Del 1
Del 2
other
log10(gDNA)
C
CRISPR-Cas9
Template oligo with alternative allele
rs139141690-A
sgRNA Del upstream
sgRNA Del downstream
Differentiation to CD41+ cells
K-562
PMA
CD41+ CD235
GG (x3)
AA (x3)
Del80 (x3)
16 24 48 72
Time (hours)
G/G
27.7
14.9
41.5
15.9
A/A
5.34
43.5
10.9
40.3
Del80
4.13
41.2
18.1
36.6
CD235-
CD41+
D
PMA treatment (hours)
Basal
16
24
48
72
Percentage of cells
G/G
A/A
Del80
CD41-CD235-
CD41+CD235+
CD41-CD235+
CD41+CD235-
E
ILR compositional model
-Log10P
Comparison
homALT vs wt
80bp del vs wt
homALT vs 80bp del


A
11 K-562 clone lines
Differentiation to CD41⁺ cells
WTA
WTB
WTC
HET
KI13
KI27
KI29
Del16
DEL233
DEL235
DEL287
EGFP
barcode #1
barcode #2
barcode #3
barcode #4
barcode #5
barcode #6
barcode #7
barcode #8
barcode #9
barcode #10
barcode #11
+ PMA
CD41⁺ CD235⁻ cells
G/G
A/G
A/A
16 bp Deletion
80 bp Deletion
Time (hours) 24 48 72 96
10X multiome
B
wnnUMAP 1
wnnUMAP 2
G/G n=2663
A/G n=1878
A/A n=1326
Del16 n=2575
Del80 n=2808
Percentage of cells
Cluster ID
1 n= 2811
2 n= 1737
3 n= 1584
4 n= 1552
5 n= 1052
6 n= 764
7 n= 473
8 n= 305
9 n= 261
10 n= 261
11 n= 241
12 n= 121
13 n= 88
C
G/G cells n=2663
ITGA2B
GYPA
IL33
IL1B
CCR7
FYB1
GP6
HBA2
HBZ
HBQ1
KIF15
STIL
ANAPC7
Cluster ID
% of cells positive
Av. Exp. scaled
Flow Cyt. Markers
Mye. Leukemia markers
Megak. markers
Hb genes
Megak. polyploid.
D
Cluster ID:
DE
DA
Comparison -log10pval
G/G vs A/G
G/G vs A/A
G/G vs 16 bp Del
G/G vs 80 bp Del
log2FoldChange
CUX1 and CUX1 target genes
AKT/mTOR signaling genes
Genes controlling Platelet volume
Platelet marker genes
Genes up-regulated in megakaryo-erythrocyte progenitors
EZH2 and target genes
E
rs139141690 G >A
CUX1
Genes
ATAC peaks
Co-expression/ co-accessibility links
Peak 2
TSS
Peak 1 & 2
Peak 3
Peak 5
Peak 7
101686267
102284958
Co-expression/ co-accessibility Links Z-score
Cluster 3 (cpm)
Cluster 1 (cpm)
Time (hours)
Genotype: G/G A/G A/A Del16 Del 80
F
CD41+CD235- cells
FSC-A
SSC-A
density
Genotype G/G A/A Del80

Rsid	chr:pos ref > alt[1]	Mechanism	Candidate gene	GWAS traits	GWS trait lineages
rs147176673[2]	chr1:202,129,205 G>A	DE	*PTPN7*	MSCV; PLT#; PCT; BASO%	ERY; MK
rs115820925	chr1:29,217,311 G>A	ATU	*EBP41*	MRV	ERY
rs12733073[3]	chr1:198,680,015 G>A	DE	*PTPRC*	MONO%; LYMPH#; LYMPH%; WBC#	LYMPH
rs150649461[2,3]	chr1:92,925,654 G>C	DE + ATU	*EVI5, GFI1*[5]	MONO#; MONO%; LYMPH%; WBC#	GM
rs140397066	chr2:144,162,105 A>G	DE	*ARHGAP15*	PDW; MONO#; NEUT%; LYMPH#; LYMPH%; WBC#	MK; GM; LYMPH
rs183347927	chr2:74,920,648 G>A	DE	*DOK1, WBP1*[5]	MPV	MK
rs114050631[3]	chr2:219,020,958 C>T	DE	*CXCR2*	MONO%; NEUT#; NEUT%; BASO#; LYMPH%; WBC#	GM
rs191451841	chr3:128,317,978 C>T	ATU	*GATA2*[5]	EO#; EO%	GM
rs112097551	chr3:128,322,617 G>A	ATU	*EEFSEC*	MCV; MCH; MSCV; MONO#; MONO%; EO#; EO%	ERY; GM
rs116577908	chr3:17,098,399 A>G	ATU	*PLCL2*	RBC#; MCV; MCH; RDW; MRV; MSCV	ERY
rs182089148	chr3:46,354,444 C>T	DE	*CCR2*	MONO#; MONO%	GM
rs35592432	chr3:71,355,240 G>C	DE + ATU	*FOXP1-IT1*[5]*, FOXP1*[5]	NEUT%; LYMPH#; LYMPH%	LYMPH
rs187282666	chr5:1,093,511 G>A	DE	*SLC12A7*	MCHC; RDW	ERY
rs186272630[3]	chr5:35,476,470 G>T	DE	*PRLR*	MONO#; MONO%	GM
rs139141690	chr7:101499930 G>A	DE	*CUX1*[5]	RET#; RET%; HLSR#; HLSR%;MPV;PDW;PCT	ERY; MK
rs149489081[4]	chr8:41589736 T>G	ATU	*ANK1*	MCV; MCHC; RDW; RET#; RET%; HLSR#; HLSR%; MRV; MSCV	ERY
rs149678861	chr15:65,174,494 A>G	DE	*ZNF609*[5]*, PLEKHO2*	PDW	MK
rs112401631	chr17:38,764,524 T>A	DE + ATU	*CCR7*	EO#;EO%; LYMPH#; LYMPH%	GM; LYMPH
rs17758695	chr18:60,920,854 C>T	ATU	*BCL2*[5]	RBC#; MCV; MCH; MRV; MSCV; PLT#; MPV; PCT; MONO#; MONO%; NEUT#; BASO#; BASO%; EO#; EO%; WBC#	ERY; MK; GM
rs17242843	chr19:11,210,157 C>T	DE	*EPOR, DOCK6*	RDW; MSCV	ERY
rs569022307	chr19:15,653,669 T>C	ATU	*RASAL3*	LYMPH#	LYMPH
rs62237617	chr22:28761148 C>T	DE	*CHEK2*	PCT; LYMPH#	MK; LYMPH

Table 1. Variants with curated mechanistic hypothesis. *For the abbreviations of blood phenotypes see Table S3. DE = Differential Expression, ATU = Alternative Transcript Usage. MK* = megakaryocytic; ERY = erythroid; LYMPH = lymphocyte; GM = granulocyte monocyte. **Trait pleiotropy: No = Lineage restricted, Yes = Multi lineage**

[1] Genomic coordinates are in the GRCh37/hg19 assembly

[2] Described as eQTL for the candidate gene in the BluePrint Consortium

[3] Described as eQTL for the candidate gene in the eQTLGen Consortium

[4] Described as sQTL for the candidate gene in the INTERVAL RNA-seq work

[5] Transcription factor or protein known to regulate gene expression